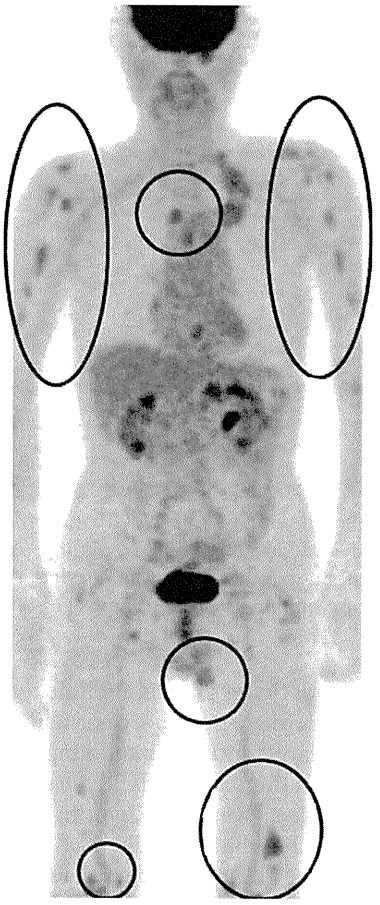

Fig 3. A positron emission tomography scan reveals extensive high-density areas in the bone and in the subcutaneous tissue of the trunk and the extremities, suggesting multiple metastases.

measuring 20 mm in diameter on the middle aspect of his left thigh (Fig 1). A complete blood cell count and chemical analysis showed no pathologic changes. Histopathologic examination of a skin biopsy specimen revealed a dense, nodular, diffuse infiltrate of monotonous uniform cells with round nuclei, prominent single or multiple nucleoli, and abundant pale, slightly eosinophilic cytoplasmic cells throughout the dermis and subcutaneous fat (Fig 2, *A*). A number of atypical mitotic figures were seen (Fig 2, *B*). The tumor cells were positive for leukocyte common antigen, CD68, and myeloperoxidase. A histologic diagnosis of myeloid leukemia cutis with possible monocytic lineage was made. However, bone marrow aspiration showed neither an increase in blasts nor abnormal cell infiltration, and repeated peripheral blood cell counts were normal, with no atypical cells. A diagnosis of ALC was established. Positron emission tomography (PET) revealed extensive high-density areas in the bone and subcutaneous tissue, suggesting multiple metastases (Fig 3). Seven weeks after his first visit, a peripheral blood cell examination disclosed 8% atypical monocytic cells, suggesting a diagnosis of acute myeloid leukemia. The patient refused other studies and died 1 week later.

ALC is a rare form of leukemia with a poor prognosis. The term "aleukemic" has been used to designate a form of leukemia in which there are no leukemic cells in the blood.[2] ALC precedes peripheral blood or bone marrow abnormalities at least 1 month before the systemic findings. Once leukemic cells appear in the peripheral blood or bone marrow, the mean survival time ranges from 3 to 30 months.[3,4] The clinical features of ALC include multiple papules, nodules, or infiltrated plaques with a red-brown or plum-colored surface. Histologic findings show the infiltration of leukemic cells in the dermal or subcutaneous tissues. The cytologic features of the tumor cells include large, vesicular nuclei and multiple prominent nucleoli.[3] Because of the rarity of the disease, there is no consensus on the treatment of choice for ALC; radiotherapy, chemotherapy, and total body electron therapy have achieved variable results.[1,3-8] A study by Chang et al[4] of a large group of ALC patients showed that the most common extramedullary site of involvement after the skin (31 of 31 patients) was the lymph nodes (8 of 31 patients) followed by the spleen (2 of 31 patients). Although no reports of a clinical presentation of ALC with multiple sites of bone infiltration were found in a thorough search of the English-language literature, extramedullary leukemia is known to occur in bone.[5] We emphasize that the routine assessment of a patient with ALC should include systemic investigations such as PET, taking into consideration the possibility of bone involvement.

Maria Maroto Iitani, MD, MSc,[a] Riichiro Abe, MD, PhD,[a] Teruki Yanagi, MD,[a] Asuka Hamasaka, MD, PhD,[a] Yasuki Tateishi, MD, PhD,[a] Yukiko Abe, MD, PhD,[a] Miki Ito, MD,[b] Takeshi Kondo, MD, PhD,[c] Kanako Kubota, MD, PhD,[d] and Hiroshi Shimizu, MD, PhD[a]

Departments of Dermatology, Hokkaido University Graduate School of Medicine[a] and the National Hospital Organization Hokkaido Cancer Center[b]; Departments of Gastroenterology and Hematology,[c] Hokkaido University Graduate School of Medicine; and the Department of Surgical Pathology,[d] Hokkaido University Hospital, Sapporo, Japan

Funding sources: None.

Conflicts of interest: None declared.

Reprint requests: Maria Maroto Iitani, MD, MSc, Department of Dermatology, Hokkaido University Graduate School of Medicine, North 15, West 7, Kita-ku, Sapporo 060-8638, Japan.

E-mail: miitani@med.hokudai.ac.jp

REFERENCES

1. Ohno S, Yokoo T, Ohta M, Yamamoto M, Danno K, Hamato N, et al. Aleukemic leukemia cutis. J Am Acad Dermatol 1990;22 (2 pt 2):374-7.
2. Yoder FW, Shuen RL. Aleukemic leukemia cutis. Arch Dermatol 1976;112:367-9.
3. Okun MM, Fitzgibbon J, Nahass GT, Forsman K. Aleukemic leukemia cutis, myeloid subtype. Eur J Dermatol 1995;5:290-3.
4. Chang H, Shih LY, Kuo TT. Primary aleukemic myeloid leukemia cutis treated successfully with combination chemotherapy: report of a case and review of the literature. Ann Hematol 2003;82:435-9.
5. Lee B, Fatterpekar GM, Kim W, Som PM. Granulocytic sarcoma of the temporal bone. AJNR Am J Neuroradiol 2002;23:1497-9.
6. Török L, Lueff S, Garay G, Tápai M. Monocytic aleukemic leukemia cutis. J Eur Acad Dermatol Venerol 1999;13:54-8.
7. Tomasini C, Quaglino P, Novelli M, Fierro MT. "Aleukemic" granulomatous leukemia cutis. Am J Dermatopathol 1998;20:417-21.
8. Imanaka K, Fujiwara K, Satoh K, Kuroda Y, Takahashi M, Sadatoh N, et al. A case of aleukemic monocytic leukemia cutis treated with total body electron therapy. Radiat Med 1988;6:229-31.

doi:10.1016/j.jaad.2009.05.040

Onychopapilloma presenting as longitudinal leukonychia

To the Editor: Onychopapilloma is an uncommon benign nail neoplasm characterized histologically by distal subungal hyperkeratosis and nail matrix metaplasia of the nail bed with marked papillomatosis. The majority of cases present clinically as localized longitudinal erythronychia. We report a case of onychopapilloma presenting as localized longitudinal leukonychia.

A 50-year-old woman was referred for the evaluation of dystrophy of the right third fingernail. The nail plate had split distally for several years. Her medical history was noncontributory. The physical examination revealed a 1-mm wide band of longitudinal leukonychia with a slight longitudinal ridge on the right third fingernail. No erythronychia was present. Distally, there was a V-shaped notch and split, with a keratotic 1-mm papule at the hyponychium (Fig 1). The other nails were normal. Lateral nail plate curl avulsion exposed a longitudinal ridge extending from the midmatrix onto the nail bed. A longitudinal biopsy from matrix to hyponychium was performed. On histologic examination, the nail bed exhibited slender, elongated, and hyperplastic rete ridges with underlying fibrosis and thickening of the fibrovascular dermal stroma. Upper nail bed keratinocytes were large and exhibited ample pink cytoplasm similar to the nail matrix keratogenous zone. Hyperkeratosis was seen at the hyponychium (Fig 2). A periodic acid–Schiff test did not reveal fungal elements. These findings were consistent with the diagnosis of onychopapilloma.

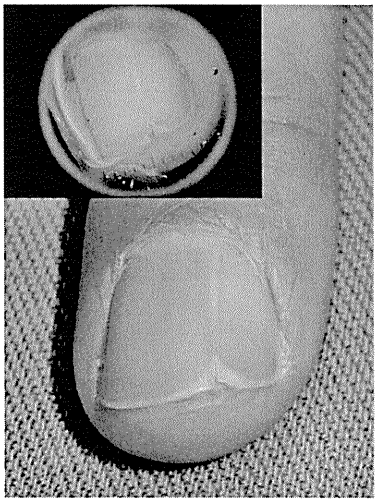

Fig 1. Fingernail with a 1-mm wide band of longitudinal leukonychia and distal V-shaped splitting, onycholysis, and a keratotic papule at the free edge of the nail. Dermatoscopy highlights these findings (*inset*).

Onychopapilloma was first reported in 1995 by Baran and Perrin,[1] who described four cases of "distal subungual keratosis with multinucleate cells." The term "onychopapilloma" was later coined in 2000 when the authors reported a second series of 14 cases with similar clinical and histopathologic features.[2] Key among these features were the upper cell layers in the nail bed epithelium exhibiting abundant eosinophilic cytoplasm resembling the nail matrix keratogenous zone, and was thought to indicate matrix metaplasia of the nail bed epithelium. Additional findings included acanthosis and papillomatosis of the distal nail bed epithelium. Multinucleated cells were found variably. In both series, all lesions presented as either longitudinal erythronychia or longitudinal bands of splinter hemorrhages, several of which were associated with distal onycholysis. Other occurrences of suspected onychopapilloma have been reported, including one case representing solitary nail bed lichen planus, and also in the spectrum of localized longitudinal erythronychia.[3] In addition to onychopapilloma, the differential diagnosis for localized longitudinal erythronychia includes Bowen disease,[2,3] and histologic investigation is often warranted.

Squamous Cell Carcinoma in a Chronic Genital Ulcer in Behçet's Disease

Hiroo Hata, Satoru Aoyagi, Maria Maroto Iitani, Erina Homma and Hiroshi Shimizu
Department of Dermatology, Hokkaido University Graduate School of Medicine, Kita-ku, Sapporo 060-8638, Japan. E-mail: hata07@med.hokudai.ac.jp
Accepted March 30, 2010.

Behçet's disease (BD) is a chronic inflammatory disease characterized by oral aphthae, genital ulcers, non-bacterial folliculitis, erythema nodosum and uveitis. The genital ulcers are characterized by clear demarcation, great depth and pain. They heal and recur, leaving scarring. In a chronic BD ulcer, squamous cell carcinoma (SCC) may develop at the scar site, as is the case with other chronic ulcers that are predisposed to malignancy. However, no cases have been reported in which SCC *in situ* has developed on a chronic genital ulcer in a patient with BD. We describe such a case here.

CASE REPORT

A 74-year-old woman presented with a 2-year history of erosive plaques in the genital region. The lesions had gradually enlarged during the previous 6 months. She had a 20-year history of repeated oral aphthae, genital ulcers and erythema nodosum. BD had been diagnosed 20 years previously. Oral corticosteroids (10 mg/day) had been administered since the initial diagnosis. Furthermore, 6 years prior to presentation, SCC had been observed on her buccal mucosa, for which she had received radiation therapy. No local recurrence had been observed.

Upon physical examination, pale-red, well-demarcated, flatly elevated lesions were extensively found symmetrically on the labia majora. The lesions were partially papillomatous and erosive (Fig. 1). Clinically, the vaginal and urethral mucosa showed no evidence of tumour spreading.

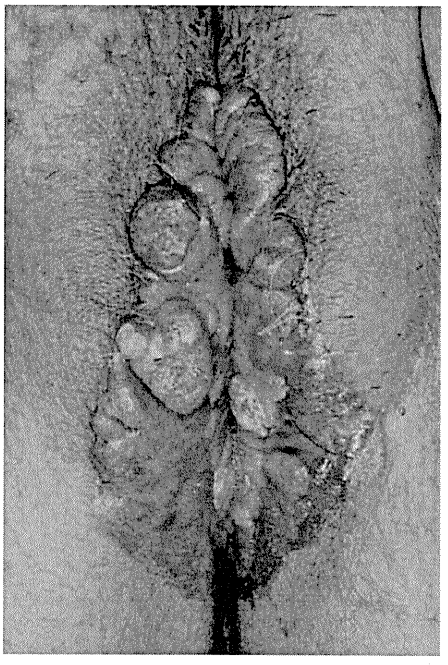

Fig. 1. Clinical features of the tumour. Well-demarcated, slightly reddish, partly papillomatous tumour presents, mainly on the labia majora.

A punch biopsy from the large plaque on the right labium majus showed proliferation of atypical keratinocytes within the acanthotic epidermis; however, the epidermal basement membrane was unaffected.

Routine laboratory examinations including that of serum SCC antigen were normal. Additionally, a computed tomography scan showed no evident distant metastasis, including of the regional lymph nodes. Therefore, the lesion was excised with at least a 1-cm margin. The surgical specimen showed neoplastic proliferation of squamous differentiated tumour cells with dyskeratotic and atypical keratinocytes (Fig. 2a). There was no evidence of dermal invasion by tumour cells (Fig. 2b). The tumour cells tested negative for anti-human papillomatous virus (HPV) antibody by immunostaining; furthermore, HPV DNA was not detected by PCR. We diagnosed this case as SCC *in situ*. The patient was disease-free 6 months after surgery with no recurrence or metastasis.

DISCUSSION

It is extremely rare for a cutaneous neoplasm to develop in cases of BD (1). To the best of our knowledge, only one such case has been reported, in which a patient with BD subsequently developed a Merkel cell carcinoma on the left forearm (2). The authors of that report suggested that immunosuppression due to the treatment for BD might have triggered the Merkel cell carcinoma, although the occurrence of BD with solid tumours tends to be regarded as coincidental.

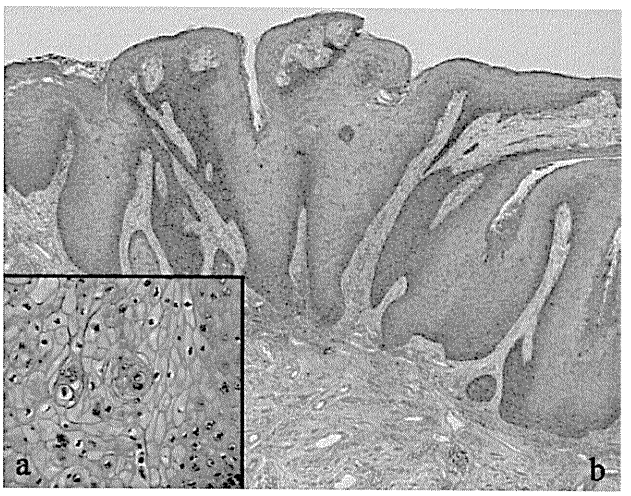

Fig. 2. (a) Neoplastic proliferation of squamous differentiated tumour cells with dyskeratotic and atypical keratinocytes only in the epidermis. These typical keratinocytes and mitoses are scattered throughout the all layers (haematoxylin and eosin; H&E). (b) There is no evidence of dermal invasion by tumour cells (H&E).

 doi: 10.2340/00015555-0902
 ISSN 0001-5555

Conditions known to be associated with increased risk of SCC *in situ* include therapeutic immunosuppression, arsenic exposure, irradiation, burn scarring, and HPV infection. In addition, HPV infection has been identified in erythroplasia of Queyrat, an intraepidermal carcinoma of the penis (3).

In our case, the refractory genital ulcer and long-term administration of oral corticosteroids may have contributed to the development of the SCC. Interestingly, our case also had a history of SCC on the buccal mucosa. The incidence of SCC *in situ* in patients with BD may be rarer than that in lichen planus or lichen sclerosis et atrophicus patients, given that similar cases have not been reported in patients with BD.

REFERENCES

1. Mansur AT, Kocaayan N, Serdar ZA, Alptekin F. Giant oral ulcers of Behçet's disease mimicking squamous cell carcinoma. Acta Derm Venereol 2005; 85: 532–534.
2. Satolli F, Venturi C, Vescovi V, Morrone P, Panfilis GD. Merkel-cell carcinoma in Behçet's disease. Acta Derm Venereol 2005; 85: 79.
3. Arlette JP. Treatment of Bowen's disease and erythroplasia of Queyrat. Br J Dermatol 2003; 149: 43–47.

severe chronic upper airway disease (SCUAD). J Allergy Clin Immunol 2009;124: 428-33.
4. Okano M, Fujiwara T, Haruna T, Kariya S, Makihara S, Higaki T, et al. PGE_2 suppresses staphylococcal enterotoxin-induced eosinophilia-associated cellular responses dominantly via an EP2-mediated pathway in nasal polyps. J Allergy Clin Immunol 2009;123:868-74.
5. Bachert C, Zhang N, van Zele T, Gevaert P, Patou J, van Cauwenberge P. *Staphylococcus aureus* enterotoxins as immune stimulants. In: Halilos DL, Baroody FM, editors. Chronic rhinosinusitis. Pathogenesis and medical management. New York: Informa Healthcare USA; 2007. p. 163-75.
6. Napolitani G, Acosta-Rodriguez EV, Lanzavecchia A, Sallusto F. Prostaglandin E_2 enhances Th17 responses via modulation of IL-17 and IFN-γ production by human CD4+ T cells. Eur J Immunol 2009;39:1-12.
7. Saito T, Kusunoki T, Yao T, Kawano K, Kojima Y, Miyahara K, et al. Role of interleukin-17A in the eosinophil accumulation and mucosal remodeling in chronic rhinosinusitis with nasal polyps associated with asthma. Int Arch Allergy Jmmunol 2009;151:8-16.
8. Su YC, Rolph MS, Hansbro NG, Mackay CR, Sewell WA. Granulocyte-macrophage colony-stimulating factor is required for bronchial eosinophilia in a murine model of allergic airway inflammation. J Immunol 2008;180:2600-7.
9. Doganci A, Eigenbrod T, Krug N, De Sanctis GT, Hausding M, Erpenbeck VJ, et al. The IL-6R alpha chain controls lung CD4+CD25+ Treg development and function during allergic airway inflammation in vivo. J Clin Invest 2005; 115:313-25.

Available online July 12, 2010.
doi:10.1016/j.jaci.2010.05.014

Topical application of dehydroxymethylepoxyquinomicin improves allergic inflammation via NF-κB inhibition

To the Editor:

Atopic dermatitis (AD) is a chronic, relapsing inflammatory skin disease with significant morbidity and an adverse impact on patient well-being. AD has become increasingly prevalent in industrialized countries, where it now occurs in 10% to 20% of children and 1% to 3% adults.[1] Corticosteroids are generally prescribed to control the symptoms, yet repeated use can cause severe skin atrophy and susceptibility to infection.[2] Tacrolimus, a calcineurin inhibitor, has recently gained widespread use as an AD treatment that avoids the typical side effects associated with topical corticosteroids.[3] However, refractory AD can remain even in patients treated with both corticosteroid and tacrolimus.

Dehydroxymethylepoxyquinomicin (DHMEQ), a newly developed low-molecular-weight nuclear factor- κB (NF-κB) inhibitor, is a 5-dehydroxymethyl derivative of the antibiotic epoxyquinomicin C.[4] DHMEQ has been found to inhibit TNF-α–induced NF-κB activation by suppressing nuclear translocation but not IκB phosphorylation or degradation.[5] Recently the antitumor effects of DHMEQ on breast,[6] thyroid,[7] and prostate[8] cancers as well as its anti-inflammatory and immunosuppressive effects have been reported in mice models.[9,10] In this study, we used atopic dermatitis model mice to examine the antiallergic inflammation efficacy of DHMEQ.

We confirmed that DHMEQ effectively inhibited the NF-κB activity in macrophage-like cell line, RAW264.7 with LPS stimulation (Fig 1, *A*).

First we examined whether DHMEQ suppressed contact hypersensitivity response. Balb/c mice were sensitized with 2,4,6-trinitrochlorobenzene (TNCB) to the dorsal skin and challenged 5 days later on the dorsal surface of the right ear. Immediately after the challenge, DHMEQ (1 mg/mL in acetone) or tacrolimus ointment (1%) was applied to the same ear. The DHMEQ-treated ears showed significantly less ear swelling than the tacrolimus-treated ears (Fig 1, *B*). The suppressive effect of DHMEQ was dose-dependent (Fig 1, *C*). Furthermore, expression of inflammatory cytokine mRNA (IL-1β, IL-6, TNF-α) in lesional skin was suppressed by DHMEQ ointment as well as by tacrolimus ointment (Fig 1, *D*). These data show that DHMEQ suppresses inflammation via suppression of inflammatory cytokine expression regulated by NF-κB.

We next examined whether DHMEQ would inhibit hapten-induced Langerhans cell (LC) migration. Treatment with TNCB caused a significant decline in epidermal LC density 4 hours after application in the untreated mice (30.5%). In contrast, TNCB treatment failed to provoke a significant epidermal LC migration response in the DHMEQ-treated mice (13.1%; Fig 1, *E*). We further evaluated LC morphology in the epidermal sheet preparations derived from the untreated and DHMEQ-treated mice. As illustrated in Fig 1, *F (left)*, at 4 hours after exposure to TNCB, the LCs in the control mice appeared to be activated and to have extended dendritic processes, whereas no such morphologic changes were evident in the LCs examined in the DHMEQ-treated mice (Fig 1, *F, right*). These data support that the DHMEQ suppressed the contact hypersensitivity response at least in part by inhibition of LC migration.

To determine whether DHMEQ has any therapeutic effect in AD, we applied DHMEQ to AD-like lesions of NC/Nga mice and evaluated the progression of skin changes. NC/Nga mice were the spontaneous mouse models of AD. Another spontaneous mouse model, the DS-Nh mouse, has a mutation of transient receptor potential vanilloid 3,[11] whereas the genetic defect of NC/Nga is not known. We used conventional NC/Nga mice that presented severe skin lesions very similar to those of human AD.[12] Conventional NC/Nga mice with moderate to severe AD were topically applied with 1% DHEMQ in plastibase (5% polyethylene and 95% mineral oil), 0.1% tacrolimus ointment, or 0.12% betamethasone ointment daily for 2 weeks. The clinical severity of skin lesion was scored daily according to the 5 main clinical symptoms: scratch behavior, erythema/hemorrhaging, edema, excoriation/erosion, and scaling/dryness.[12] Topical DHMEQ application significantly improved the severity of skin lesions compared with the ointment base as well compared with topical treatment with the 0.1% tacrolimus or 0.12% betamethasone ointment (Fig 2, *A and B*). Improvement of clinical skin condition by DHMEQ was also confirmed by histologic observation, which showed amelioration of hyperkeratosis, acanthosis, dermal edema, and infiltration of the inflammatory cells compared with the ointment base treatment (Fig 2, *C*). At the affected skin sites, the numbers of eosinophils and mast cells were significantly lower in the DHMEQ-treated mice than those in the control mice (Fig 2, *C*).

Potential side effects of topical application of NF-κB inhibition might include susceptibility to infection via local immune suppression. However NF-κB inhibitor presumably avoids the typical side effects associated with topical corticosteroids as well as tacrolimus.

Several reagents targeting NF-κB have been reported. For example, NF-κB decoy oligodeoxynucleotides were reported to be effective in resolving atopic skin lesions in NC/Nga mice.[13] IMD-0354, a selective IKK inhibitor, also improved AD manifestation in model mice.[14] In contrast with these, DHMEQ inhibits NF-κB activation by suppressing nuclear translocation but not IκB phosphorylation or degradation.[5] Because DHMEQ has a unique mechanism to inhibit NF-κB activation, DHMEQ might be effective for AD that does not respond to tacrolimus or corticosteroid, and it might have additive effects with other reagents.

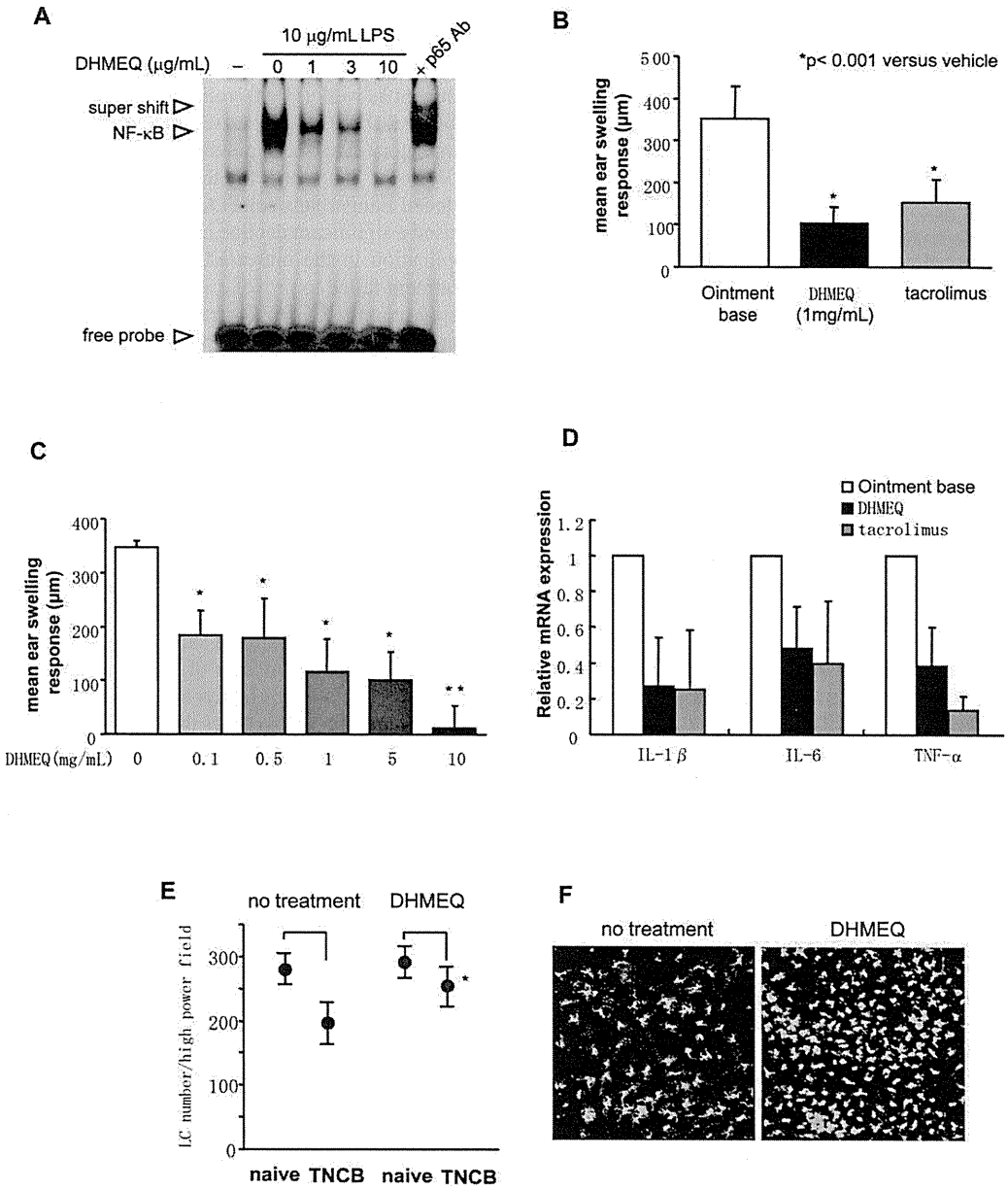

FIG 1. Effect of DHMEQ on contact hypersensitivity response. **A,** DHMEQ effectively inhibited the NF-κB activity in macrophagelike cell line RAW264.7 with LPS stimulation (10 μg/mL). **B,** DHMEQ, tacrolimus, or ointment base was applied topically. All ear-swelling values are shown as means ± SEs (n = 5). $*P < .01$; $**P < .005$. **C,** DHMEQ was applied in various concentrations. **D,** The density of mRNA expression of skin was analyzed by RT-PCR. **E,** The number of LCs was counted. $*P < .05$ (n = 4 for each group). **F,** LC morphology in epidermal sheet preparations derived from untreated *(left)* and DHMEQ-treated *(right)* mice.

In conclusion, we clearly demonstrated that DHMEQ inhibits the contact hypersensitivity response via suppression of inflammatory cytokines and decrease in LC migration. Furthermore, DHMEQ was found to improve AD manifestation of model mice with an efficacy equivalent to that of tacrolimus or betamethasone. DHMEQ may offer a novel therapeutic approach for the treatment of AD.

Asuka Hamasaka, MD, PhD[a]*
Naoya Yoshioka, MS[a]*
Riichiro Abe, MD, PhD[a]
Satoshi Kishino, PhD[d]
Kazuo Umezawa, MD, PhD[e]
Michitaka Ozaki, MD, PhD[b]
Satoru Todo, MD, PhD[c]
Hiroshi Shimizu, MD, PhD[a]

From [a]the Department of Dermatology, [b]the Department of Molecular Surgery, and [c]the First Department of Surgery, Hokkaido University Graduate School of Medicine, Sapporo; [d]the Department of Medication Use Analysis and Clinical Research, Meiji Pharmaceutical University, Tokyo; and [e]the Department of Applied Chemistry, Keio

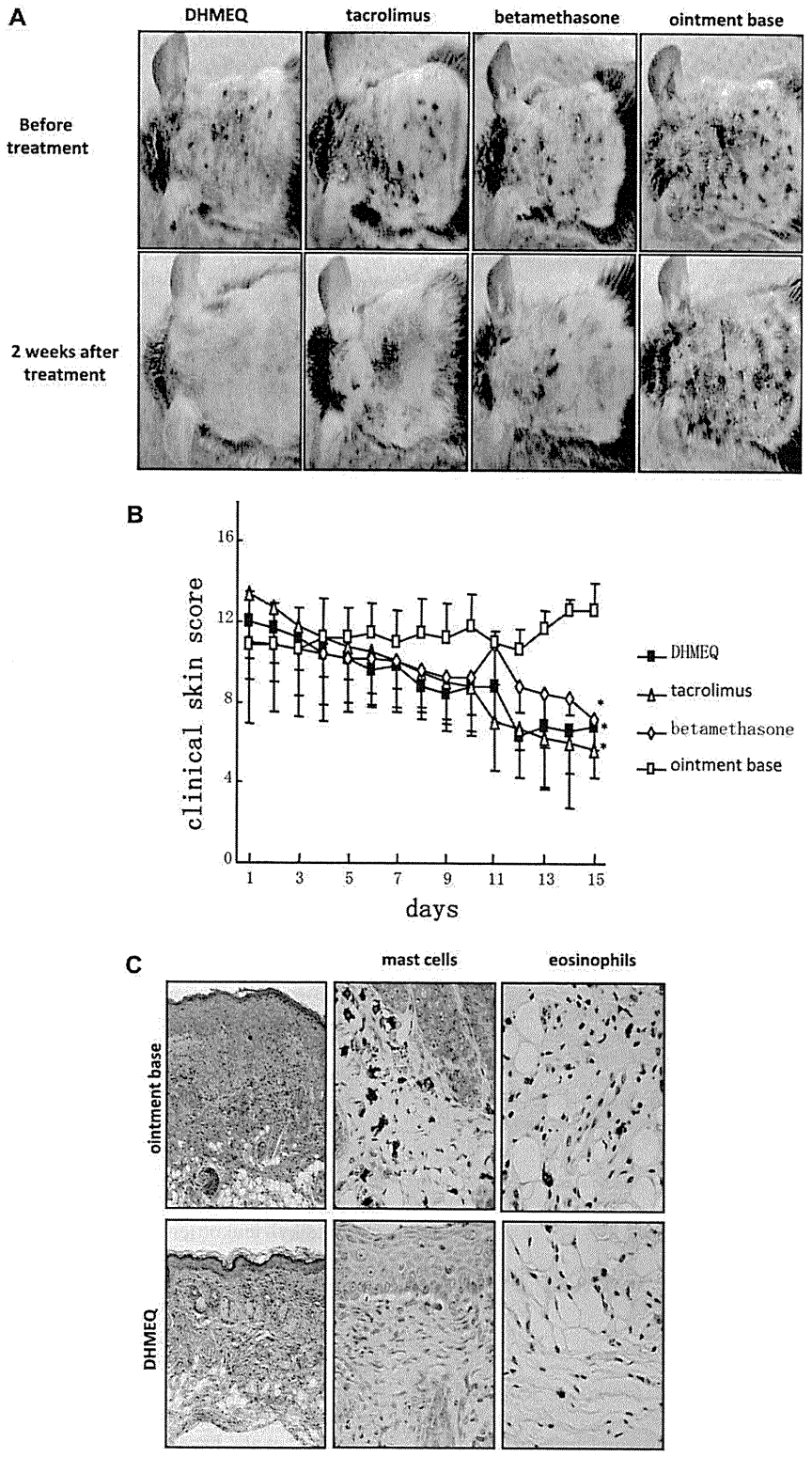

FIG 2. Improvement of atopic dermatitis model mice by DHMEQ. NC/Nga mice were applied topically with DHMEQ, tacrolimus, or ointment base. **A,** Clinical features of each mouse. **B,** The clinical skin score of each group is given as mean ± SE. $*P < .005$. **C,** Specimens were collected from the dorsal skin and were stained with hematoxylin and eosin, direct fast scarlet for eosinophils, or toluidine blue for mast cells.

University, Yokohama, Japan. E-mail: aberi@med.hokudai.ac.jp, shimizu@med.hokudai.ac.jp.

Disclosure of potential conflict of interest: This study was supported by the Program for Promotion of Fundamental Studies in Health Sciences of the National Institute of Biomedical Innovation (NIBIO).

*These authors contributed equally to this work.

REFERENCES

1. Morar N, Willis-Owen SA, Moffatt MF, Cookson WO. The genetics of atopic dermatitis. J Allergy Clin Immunol 2006;118:24-34, quiz 5-6.
2. Abramovits W, Perlmutter A. Steroids versus other immune modulators in the management of allergic dermatoses. Curr Opin Allergy Clin Immunol 2006;6: 345-54.
3. El-Batawy MM, Bosseila MA, Mashaly HM, Hafez VS. Topical calcineurin inhibitors in atopic dermatitis: a systematic review and meta-analysis. J Dermatol Sci 2009;54:76-87.
4. Matsumoto N, Ariga A, To-e S, Nakamura H, Agata N, Hirano S, et al. Synthesis of NF-kappaB activation inhibitors derived from epoxyquinomicin C. Bioorg Med Chem Lett 2000;10:865-9.
5. Ariga A, Namekawa J, Matsumoto N, Inoue J, Umezawa K. Inhibition of tumor necrosis factor-alpha -induced nuclear translocation and activation of NF-kappa B by dehydroxymethylepoxyquinomicin. J Biol Chem 2002;277: 24625-30.
6. Matsumoto G, Namekawa J, Muta M, Nakamura T, Bando H, Tohyama K, et al. Targeting of nuclear factor kappaB Pathways by dehydroxymethylepoxyquinomicin, a novel inhibitor of breast carcinomas: antitumor and antiangiogenic potential in vivo. Clin Cancer Res 2005;11:1287-93.
7. Starenki DV, Namba H, Saenko VA, Ohtsuru A, Maeda S, Umezawa K, et al. Induction of thyroid cancer cell apoptosis by a novel nuclear factor kappaB inhibitor, dehydroxymethylepoxyquinomicin. Clin Cancer Res 2004;10:6821-9.
8. Kikuchi E, Horiguchi Y, Nakashima J, Kuroda K, Oya M, Ohigashi T, et al. Suppression of hormone-refractory prostate cancer by a novel nuclear factor kappaB inhibitor in nude mice. Cancer Res 2003;63:107-10.
9. Wakamatsu K, Nanki T, Miyasaka N, Umezawa K, Kubota T. Effect of a small molecule inhibitor of nuclear factor-kappaB nuclear translocation in a murine model of arthritis and cultured human synovial cells. Arthritis Res Ther 2005;7: R1348-59.
10. Ueki S, Yamashita K, Aoyagi T, Haga S, Suzuki T, Itoh T, et al. Control of allograft rejection by applying a novel nuclear factor-kappaB inhibitor, dehydroxymethylepoxyquinomicin. Transplantation 2006;82:1720-7.
11. Asakawa M, Yoshioka T, Matsutani T, Hikita I, Suzuki M, Oshima I, et al. Association of a mutation in TRPV3 with defective hair growth in rodents. J Invest Dermatol 2006;126:2664-72.
12. Matsuda H, Watanabe N, Geba GP, Sperl J, Tsudzuki M, Hiroi J, et al. Development of atopic dermatitis-like skin lesion with IgE hyperproduction in NC/Nga mice. Int Immunol 1997;9:461-6.
13. Nakamura H, Aoki M, Tamai K, Oishi M, Ogihara T, Kaneda Y, et al. Prevention and regression of atopic dermatitis by ointment containing NF-kB decoy oligodeoxynucleotides in NC/Nga atopic mouse model. Gene Ther 2002;9: 1221-9.
14. Tanaka A, Muto S, Jung K, Itai A, Matsuda H. Topical application with a new NF-kappaB inhibitor improves atopic dermatitis in NC/NgaTnd mice. J Invest Dermatol 2007;127:855-63.

Available online July 12, 2010.
doi:10.1016/j.jaci.2010.05.020

A novel non–IgE-mediated pathway of mite-induced inflammation

To the Editor:

In a recent article published in the *Journal of Immunology*, Barrett et al[1] demonstrated that mite and *Aspergillus fumigatus* extracts stimulate the production of cysteinyl leukotrienes from bone marrow–derived dendritic and pulmonary $CD11c^+$ cells through a glycan C–type lectin receptor (Dectin-2) interaction involving FcRγ and Syk signaling that activates arachidonic acid metabolism.

Previously, a number of clinical and experimental observations had called our attention to the existence of important connections between IgE-mediated diseases and leukotriene-mediated inflammation. We had observed that a large proportion of patients with hypersensitivity to nonsteroidal anti-inflammatory drugs (NSAIDs), a condition that is accompanied by increased production of leukotrienes, were atopic and had IgE-mediated sensitivity to mite allergens.[2] This observation has been recently confirmed in another study in which we found significantly increased total and mite-specific IgE levels in patients with NSAID hypersensitivity compared with those seen in healthy control subjects.[3] In tropical countries in which high relative humidity and temperature are optimal for mite proliferation, mite allergens are the main source of sensitization and allergic respiratory disease.

A second clinical observation, also reported by Spanish investigators and others, was that most patients with anaphylaxis after the ingestion of mite-contaminated foods frequently exhibit hypersensitivity to NSAIDs.[4] We designated the association of allergic rhinitis, aspirin/NSAID hypersensitivity, and severe reactions to mite-contaminated foodstuffs as a "new aspirin triad." To understand this association, we performed a study in collaboration with Canadian investigators in which it was demonstrated that mite allergenic extracts inhibited COX-1 *in vitro*. We postulated that mite-induced human allergic diseases could be accompanied, at least in a subset of the patient population, by a dysregulation of leukotriene biosynthesis, metabolism, or both similar to the disturbances described in patients with NSAID hypersensitivity.

In concordance with that hypothesis, various genetic polymorphisms that involve leukotriene C_4 (LTC_4) synthase and cysteinyl leukotriene receptors have been observed in patients with hypersensitivity to NSAIDs; in that context it is important to mention that so-called atopic genes are located in the 5q22-q35 region of human chromosome 5, close to the *LTC4S* gene.

Diverse lines of evidence also support a dysregulation of leukotriene pathways in subjects with mite allergy. Acevedo et al[5] described an association of the A-444C allele of the *LTC4S* gene and IgE response to mite allergens, and we have observed that NSAID-sensitive patients show stronger skin test responses and increased specific IgE antibodies to *Blomia tropicalis* than atopic non–NSAID-sensitive subjects.[3]

Cysteinyl leukotrienes modulate the allergic response, as evidenced in various studies in which it has been shown that leukotrienes enhance IgE and IgG production by human B cells, whereas *LTC4S* knockout mice have a markedly reduced antigen-induced T_H2 pulmonary inflammation. Additionally, it has been demonstrated that IL-4 and IL-13 modulate the number of cysteinyl leukotriene type 1 and 2 receptors on T, B, and antigen-presenting cells.

Furthermore, various groups of investigators have observed that aspirin enhances food-dependent exercise-induced anaphylaxis[6] and facilitates anaphylaxis induced by food allergens.[7-10] These effects could be due to an increased gut permeability, resulting in enhanced opportunity for sensitization at the immunocompetent cell–rich gastrointestinal submucosa.

Bachert et al[11] have proposed a role for staphylococcal enterotoxins, which, through the Vβ receptor on T lymphocytes, allow polyclonal IgE production, including IgE to house dust mite, in nasal polyps, the lungs, and possibly the skin. It would be interesting to investigate in the future whether aspirin-hypersensitive patients with urticaria and angioedema and those with oral anaphylaxis to mites have superantigen-induced immune stimulation

Bone marrow transplantation restores epidermal basement membrane protein expression and rescues epidermolysis bullosa model mice

Yasuyuki Fujita[a], Riichiro Abe[a,1], Daisuke Inokuma[a], Mikako Sasaki[a], Daichi Hoshina[a], Ken Natsuga[a], Wataru Nishie[a], James R. McMillan[a], Hideki Nakamura[a], Tadamichi Shimizu[b], Masashi Akiyama[a], Daisuke Sawamura[c], and Hiroshi Shimizu[a,1]

[a]Department of Dermatology, Hokkaido University Graduate School of Medicine, Sapporo 060-8638, Japan; [b]Department of Dermatology, Toyama University Graduate School of Medicine and Pharmaceutical Sciences, Toyama 930-0194, Japan; and [c]Department of Dermatology, Hirosaki University Graduate School of Medicine, Hirosaki 036-8562, Japan

Edited* by Douglas Lowy, National Institutes of Health, Bethesda, MD, and approved June 24, 2010 (received for review January 4, 2010)

Attempts to treat congenital protein deficiencies using bone marrow-derived cells have been reported. These efforts have been based on the concepts of stem cell plasticity. However, it is considered more difficult to restore structural proteins than to restore secretory enzymes. This study aims to clarify whether bone marrow transplantation (BMT) treatment can rescue epidermolysis bullosa (EB) caused by defects in keratinocyte structural proteins. BMT treatment of adult collagen XVII (Col17) knockout mice induced donor-derived keratinocytes and Col17 expression associated with the recovery of hemidesmosomal structure and better skin manifestations, as well improving the survival rate. Both hematopoietic and mesenchymal stem cells have the potential to produce Col17 in the BMT treatment model. Furthermore, human cord blood CD34$^+$ cells also differentiated into keratinocytes and expressed human skin component proteins in transplanted immunocompromised (NOD/SCID/γ_c^{null}) mice. The current conventional BMT techniques have significant potential as a systemic therapeutic approach for the treatment of human EB.

hematopoietic stem cells | type XVII collagen

Bone marrow-derived cells, including hematopoietic stem cells and mesenchymal stem cells, have been reported to play a significant role in the recovery of various impaired organs (1–8). Although some papers have reported that "transdifferentiation" of circulating hematopoietic stem cells is an extremely rare event (9), previous reports have shown that expression of systemic enzymes and certain secreted factors can be recovered after bone marrow transplantation (BMT) (10).

Epidermolysis bullosa (EB) comprises a group of genodermatoses, which are caused by mutations in one of the genes encoding anchor proteins that stabilize the basement membrane zone (BMZ) of the skin and mucous membranes (11). Collagen XVII (COL17) is a transmembrane component of hemidesmosomal adhesion structures anchoring cells to the BMZ. *COL17* is the gene underlying non-Herlitz junctional EB in humans, a disorder that causes severe skin fragility, hair loss, growth retardation, and enamel hypoplasia (11). There is no effective treatment for EB other than palliative care. Gene-treated cultured autografting, reported by Mavilio et al. (12), is a promising therapeutic approach for junctional EB. However, its effects are limited to the area of application, in addition to the ethical and safety problems of using viruses for gene correction, even if the recent development of lentiviral vectors with favorable safety might be able to avoid the risks of gene augmentation with traditional retroviral constructs (13). Therefore, systemic and ethically safer therapies would be preferable.

Previous work reported that cells of human or murine origin do home to the skin, such as in graft-versus-host disease in humans (14) and epithelial progenitors in murine bone marrow (15). Our group reported that donor-derived keratinocytes could be identified at wound sites in a BMT model (16). This suggests that BMT techniques have the potential to provide functional keratinocytes over the entire skin surface. The current study investigates whether BM-derived cells can differentiate into donor-derived keratinocytes and subsequently produce detectable COL17 protein after BMT, with the ultimate goal of improving the clinical phenotype and contributing to long-term survival in our model mice.

Results

Donor BM-Derived Cells Express Col17 Protein in the BMZ in Recipient Mouse Skin. To investigate whether BM-derived keratinocytes can produce skin component proteins, we transplanted BM-derived cells of C57BL/6 mice expressing *human COL17* (*hCOL17*) driven by the keratin 14 promoter (*COL17*$^{m+/+,h+}$) into wild-type C57BL/6 mice in the first set of experiments. Detection of hCOL17 protein in the epithelized recipient skin would indicate that donor BM-derived cells had differentiated into keratinocytes. Immunohistochemical analysis revealed hCOL17 protein expression in the BMZ within the wounded area for four out of the eight BMT-treated C57BL/6 mice (Fig. 1*A*). RT-PCR analysis also showed evidence of *hCOL17* mRNA expression in five out of the eight treated mice (Fig. 1*B*).

We subsequently performed another BMT experiment: BM-derived cells from GFP$^+$ Tg mice were transplanted into COL17-humanized (*COL17*$^{m-/-,h+}$) mice (Fig. S1) (17). In this experimental pattern, BM-derived cells that differentiated into keratinocytes in the host mice were found to have the potential to produce mCol17 protein. BM-derived nonhematopoietic cells expressing GFP$^+$ CD45$^-$ were sparsely observed, accounting for $1.83 \pm 0.82\%$ ($n = 5$) of the basal layer cells (Fig. 1*C*). Aggregated GFP$^+$ cytokeratin$^+$ cells were also found in the basal cell layer (Fig. 1*D*). Epithelized skin areas in this experiment demonstrated mCol17 protein expression, although unwounded areas of the transplanted *COL17*$^{m-/-,h+}$ mice failed to express that protein (Fig. 1*E*). This mCol17 expression lasted at least 9 mo after wound formation in two out of the three investigated mice (Fig. S2). RT-PCR analysis also revealed the expression of *mCol17* mRNA in epithelized skin from four of the five transplanted mice, indicating that the BM-derived epidermal cells were able to express active *mCol17* (Fig. 1*F*).

Author contributions: Y.F., R.A., D.I., W.N., T.S., M.A., D.S., and H.S. designed research; Y.F., D.I., M.S., D.H., K.N., W.N., J.R.M., H.N., and D.S. performed research; K.N. and W.N. contributed new reagents/analytic tools; and Y.F., R.A., M.S., J.R.M., M.A., and H.S. analyzed data; and Y.F. and R.A. wrote the paper.

The authors declare no conflict of interest.

*This Direct Submission article had a prearranged editor.

[1]To whom correspondence may be addressed. E-mail: aberi@med.hokudai.ac.jp or shimizu@med.hokudai.ac.jp.

This article contains supporting information online at www.pnas.org/lookup/suppl/doi:10.1073/pnas.1000044107/-/DCSupplemental.

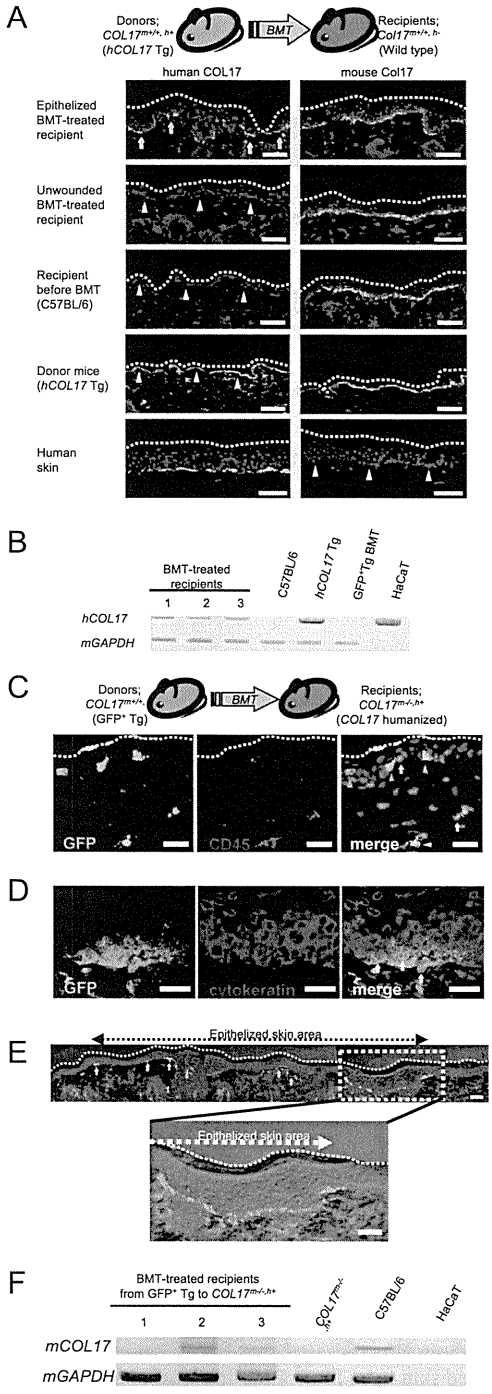

Fig. 1. BMT-induced donor cell-derived COL17 in the epithelized skin tissue. (*A*) The donor-derived hCOL17 expression is observed in the epithelized skin areas of BMT-treated C57BL/6 recipients (yellow arrows). Green: mCol17 (KT4.2) or hCOL17 (D20); red: nuclei; broken lines: skin surface; arrowheads: BMZ. (Scale bars: 50 μm.) (*B*) Representative RT-PCR analysis for *hCOL17* expression reveals positive bands in BMT-treated C57BL/6 recipients. All RNA samples were extracted from full-thickness skin biopsies, except for HaCaT from cultured cells. (*C*) Immunohistochemical analysis of the BMT-treated $COL17^{m-/-, h+}$ skin tissue demonstrates donor-derived GFP^+ $CD45^+$ blood cells (yellow arrowheads) and recipient-derived GFP^- $CD45^+$ cells (yellow arrow). Donor-derived GFP^+ $CD45^-$ (green arrowheads) cells are sporadically noted in the epidermis. (Scale bars: 20 μm.) (*D*) Aggregated donor-derived GFP^+ cells in the basal cell layer are noted, some of which also express cytokeratin (white arrows). These cells are thought to be donor-derived keratinocytes. (Scale bars: 20 μm.) (*E*) The skin of the recipients shows sporadic, linear deposition of mCol17 (arrows). The deposition is limited to the epithelized skin area with acanthosis. (*Upper*) The entire consolidated image. (*Lower*) Higher magnification. (Scale bars: 50 μm.) (*F*) RT-PCR analysis shows the recovery of *mCol17* mRNA in two out of three representative mice (lanes 2 and 3).

BM-Derived Cells Supply Deficient Col17 Protein in the Col17 Knockout EB Model Mice. Our group recently established non-Herlitz junctional EB model mice ($COL17^{m-/-}$) as a result of homozygous ablation of the Col17 gene (17). Unlike EB model mice reported by other researchers, our model has allowed us to obtain adult $COL17^{m-/-}$ mice that can be used for various therapeutic strategies (Fig. S3). We speculated that mCol17 protein would be reintroduced by administering BM-derived cells from BMT treatments into $COL17^{m-/-}$ EB model mice. We transplanted BM cells of the GFP^+ Tg mice into the $COL17^{m-/-}$ mice. All of the mice obtained hematopoietic chimeras (710. ± 4.0%, $n = 21$). Immunohistochemical analysis revealed sporadic GFP^+ cells in the basal cell layer of the epidermis, accounting for 1.08 ± 0.39% of the basal cells ($n = 11$). GFP^+ $CD45^-$ cells including cytokeratin$^+$ epidermal keratinocytes were also found (0.26% ± 0.08% of basal cells) (Fig. 2*A* and Fig. S4). Linear deposition of mCol17 along the BMZ, and GFP^+ cells above the mCol17 staining were observed, accounting for 14.7 ± 3.0% ($n = 11$) of the epithelized area (Fig. 2*B*). Also, a 180-kDa mCol17 protein was detected in Western blotting (Fig. 2*C*). One out of three mice showed positive mCol17 immunohistochemically in unwounded skin from the back (Fig. S5*A*). Eight out of nine BMT-treated mice showed positive *mCol17* mRNA in the epithelized skin tissues. Compared with unwounded skin, epithelized areas of skin tended to show *mCol17* mRNA expression more frequently (Fig. S5*B*). We also performed RT-PCR analysis on the epithelized areas of BMT-treated $COL17^{m-/-}$ mice from the epidermis and the dermis by detaching each side enzymatically; this revealed positivity only on the epidermal side (Fig. 2*D*). Next, we sorted GFP^+ cells from the single-cell suspension of epithelized epidermal cells. A portion of the suspended epidermal cells showed GFP (1.24 ± 0.12%, $n = 4$; Fig. S6), and mRNA expression specific to epidermal keratinocytes was detected from the extract of the GFP^+ epidermal cells. These cells also expressed *mCol17* mRNA in three out of the four investigated mice (Fig. 2*E*). To rule out the possibility that cell fusion was occurring between BM cells and original keratinocytes in the $COL17^{m-/-}$ mice, we performed FISH analysis in a sex-mismatched BMT model. Several fused cells with XXXY chromosomes in the same nucleus were found in the deep dermis of the epithelized skin (Fig. 2*F*). Conversely, no fused cells were found in the epidermis of the samples we investigated, whereas 50 of 1,793 basal cells (2.79%) showed donor-derived XY chromosomes. To investigate the restoration of COL17 expression and its effect on restoring normal BMZ structure, we performed electron microscopic analysis. In the BMT-treated $COL17^{m-/-}$ mice, a portion of the basal cells had mature hemidesmosomes (Fig. 2*G*). The average thickness of outer plaques of hemidesmosomes was 79.7 ± 3.2 nm in the wild-type mice, 45.1 ± 1.4 nm in the untreated $COL17^{m-/-}$ mice, and 61.1 ± 1.9 nm in the BMT-treated $COL17^{m-/-}$ mice ($P < 0.01$). To exclude the nonspecific effects of bone marrow infusion, a mixture of lineage$^+$ differentiated GFP^+ BM cells and lineage$^-$ $COL17^{m-/-}$ BM cells was transplanted into the $COL17^{m-/-}$ mice. No Col17 expression of mRNA and protein were detected in the epithelized skin ($n = 3$).

Col17 Knockout Mice Exhibit Less Severe Clinical Manifestations and Better Survival Prognosis After BMT than Untreated Mice. To investigate the change in vulnerability to friction in skin that resulted from the restoration of Col17, we rubbed the back of each mouse (18). The BMT-treated mice ($n = 6$) significantly showed formation of smaller erosions compared with the untreated mice ($n = 4$) (Fig. 3*A*). Although our $COL17^{m-/-}$ mice survived longer than previously reported EB models, only 12.5% of the mice survived to 1 mo, approximately half of which died within the following 3 mo (17). Surprisingly, 16 out of the 20 transplanted $COL17^{m-/-}$ mice survived to 100 d after BMT (transplanted on d 35 after birth), whereas only 7 out of the 17 untreated $COL17^{m-/-}$ mice survived to

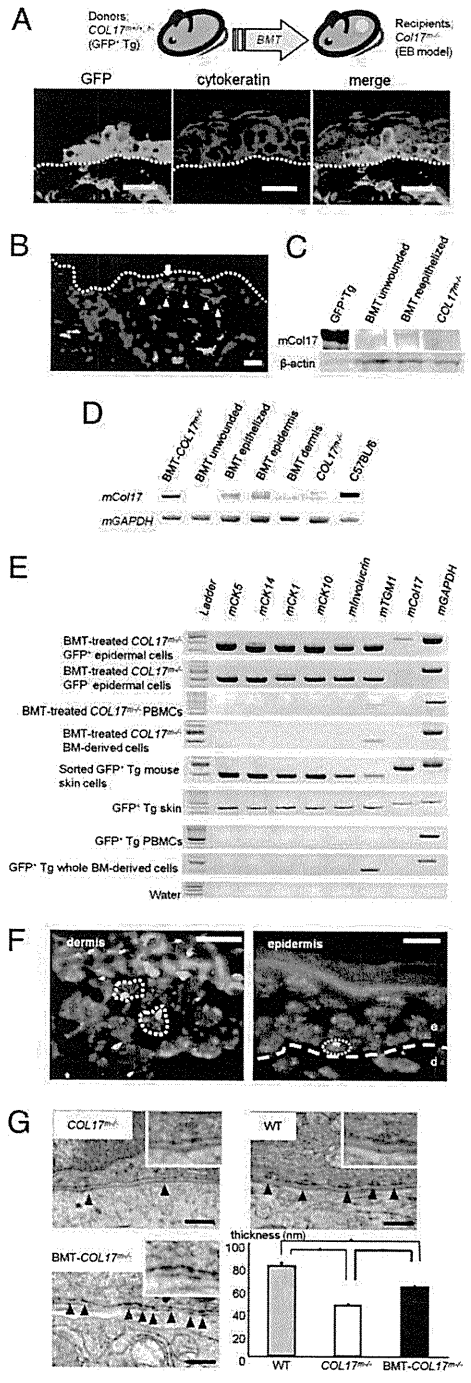

Fig. 2. BMT treatments induce functional mCol17 in *COL17*$^{m-/-}$ junctional EB model mice. (*A*) In the epithelized skin tissue of BMT-treated mice, a cluster of GFP$^+$ cytokeratin$^+$ basal cells is observed. Green: GFP; blue: nuclei; broken lines: skin surface. (Scale bars: 10 μm.) (*B*) Sporadic GFP$^+$ cells (green) are shown in the epithelized skin of the recipients (arrow). Furthermore, linear staining of mCol17 is detected in the BMZ (red, KT4.2, arrowheads). (Scale bars: 20 μm.) (*C*) Western blotting analysis reveals the expression of mCol17 in the epithelized area of the BMT-treated *COL17*$^{m-/-}$ mouse (lane 3), and a weak band is seen in unwounded skin of a BMT-treated *COL17*$^{m-/-}$ mouse (lane 2). β-actin: loading control. (*D*) The expression of *mCol17* is detected only in the epithelized skin and not in the unwounded skin area. Also, the expression is limited to the epidermis side of the epithelized skin. (*E*) The sorted GFP$^+$ single epidermal cells of BMT-treated *COL17*$^{m-/-}$ mice express various keratinocyte-specific mRNAs as well as *mCol17*. Sorted GFP$^-$ cells express these mRNAs, other than that of mCol17. (*F*) No fused cells are apparent in the epidermis, although donor-derived XY cells are sparsely shown. Sporadic fused cells with XXXY chromosomes are observed in the deep dermis. Dashed circles indicate the border of the nucleus. e: epidermis; d: dermis. (Scale bars: 10 μm.) (*G*) The epithelized skin of *COL17*$^{m-/-}$ mice has hypoplastic hemidesmosomes with thin, poorly formed inner/outer plaques (arrowheads). In BMT-treated *COL17*$^{m-/-}$ mice, hemidesmosomes with mature plaques are seen. (Scale bars: 500 nm.) *$P < 0.01$.

d 135 after birth. The survival outcomes were 73.7% for the transplanted group and 27.5% for the untreated group at d 200 after BMT (Fig. 3*B*). The BMT technique brought significant therapeutic benefits to the *COL17*$^{m-/-}$ EB model mice.

The untreated adult *COL17*$^{m-/-}$ EB model mice showed spontaneous erosions, ulcers, nail deformity, hair loss, and hair graying similar to those seen in human junctional EB patients lacking *COL17* (17). The erosions were especially severe in the genital regions (Fig. 3*C*). The BMT-treated *COL17*$^{m-/-}$ mice showed improvements to clinical manifestations, with fewer spontaneous erosions than for the untreated *COL17*$^{m-/-}$ mice and BMT-control *COL17*$^{m-/-}$ mice (*COL17*$^{m-/-}$ mice as donors). The improvements were particularly marked in the genital regions (Fig. S7).

Both Hematopoietic and Mesenchymal Stem Cells Contribute to the Expression of Col17. Because BM cells consist of various differentiated hematopoietic cells and stem cells, there is the question of which type of BM-derived stem cells produced the Col17 and caused clinical improvement in the *COL17*$^{m-/-}$ EB model mice. We obtained hematopoietic stem cells (HSCs) and multipotent mesenchymal stromal cells (MSCs) from GFP$^+$ Tg mice, following transplantation of each type of stem cell into *COL17*$^{m-/-}$ mice with whole *COL17*$^{m-/-}$ BM-derived cells as supporting cells (Fig. 4*A*). Four weeks after BMT, we confirmed partial chimerism (37.0 ± 13.7%, $n = 5$) of GFP in peripheral blood of BMT-treated mice with GFP$^+$ HSCs (HSC-BMT mice), whereas no GFP$^+$ peripheral blood cells were detected in BMT-treated mice with GFP$^+$ MSCs (MSC-BMT mice, $n = 4$) (Fig. S8). Immunohistochemical analysis revealed sparse GFP$^+$ cytokeratin$^+$ keratinocytes in the skin of the HSC- and MSC-BMT mice (Fig. 4*B*). Both HSCs and MSCs were found to have the potential to produce mCol17 as observed immunohistochemically; three out of five HSC-BMT mice and two out of four MSC-BMT mice showed positive mCol17 (Fig. 4*C*). RT-PCR analysis also demonstrated the expression of *mCol17* in both the HSC-BMT model (three out of five mice) and the MSC-BMT model (two out of four mice) (Fig. 4*D*). HSC-BMT mice showed better clinical manifestations than untreated *COL17*$^{m-/-}$ mice, whereas mice of the MSC-BMT model had a tendency to show more severe perianal erosions and hair loss (Fig. 4*E*).

Transplanted Human Cord Blood CD34$^+$ Cells Obtain a Keratinocyte-Like Phenotype and Produce Epidermal Component Proteins. Toward clinical applications of stem cell transplantation therapies in human EB patients, we investigated whether the human hematopoietic stem cells have the ability to supply structural proteins in the BMZ of the skin. A human-to-mouse xenogeneic transplantation model was investigated using NOD/SCID/γ_c^{null} (NOG) mice (19). Using immunohistochemistry, human cells that expressed human leukocyte antigen (HLA)-ABC could be seen, and pancytokeratin-positive cells were sporadically costained (0.39 ± 0.15% of the basal cells, $n = 4$) (Fig. 5*A* and *B*), which indicates that these cells are donor cell-derived keratinocytes. In addition, sparse and intermittent hCOL17 was detected along the BMZ in two of seven treated mice (Fig. 5*C*). RT-PCR analysis surprisingly showed mRNA expression of several components of the normal human BMZ other than *hCOL17* (detected in six of seven treated mice), including *BPAG1* (four of seven), *plectin* (four of seven), *α6 integrin* (five of seven), *laminin β3* (two of seven), and *laminin γ2* (one out of seven) (Fig. 5*D*).

Discussion

Junctional EB is caused by mutations in the genes coding for structural proteins anchoring the skin to the underlying basal

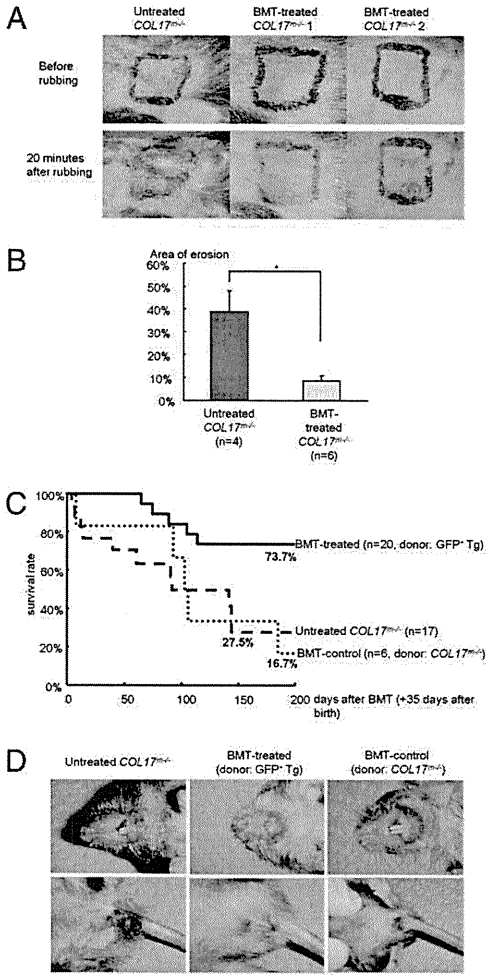

Fig. 3. BMT treatments in $COL17^{m-/-}$ junctional EB model mice change vulnerability to friction in the skin and induce better clinical conditions. (*A*) epithelized areas after erosion formation are investigated by rubber stress test. In untreated $COL17^{m-/-}$ mice, mild mechanical stimulus induces large erosions. Conversely, BMT-treated mice show less severe erosions. $*P < 0.05$. (*B*) The erosion area expressed as a percent of the rubbed area is measured for each group. Resistance of the skin to mechanical stimuli is significantly improved in the BMT-treated $COL17^{m-/-}$ mice. (*C*) Survival curves of BMT-treated and -untreated $COL17^{m-/-}$ mice from d 35 after birth (the day of BMT). $COL17^{m-/-}$ mice treated with BMT from $COL17^{m-/-}$ mice are shown as the BMT control mice; 73.7% of BMT-treated $COL17^{m-/-}$ mice could be expected to live over 200 d after BMT treatment vs. only 27.5% of untreated $COL17^{m-/-}$ mice and 16.7% of BMT control mice. ($P = 0.015$ for BMT-treated vs. untreated mice, $P = 0.021$ for BMT-treated vs. BMT control, and $P = 0.964$ for BMT control vs. untreated.). (*D*) Clinical manifestations at 90 d after BMT treatment (125 d after birth). Untreated $COL17^{m-/-}$ mice show moderate perioral erosions with crusts and anal erosions occurring spontaneously. In contrast, BMT-treated $COL17^{m-/-}$ mice show mild erosions in these areas.

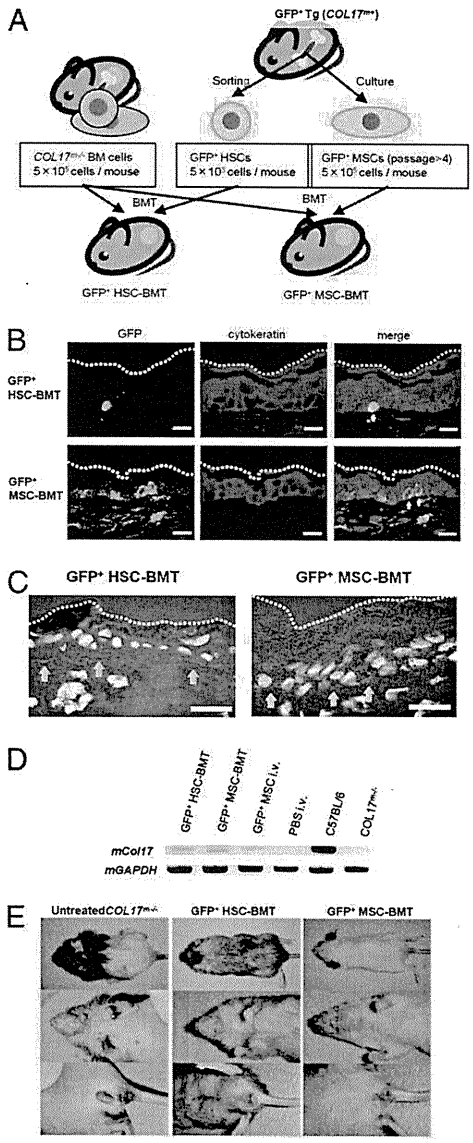

Fig. 4. HSCs and MSCs each have the potential to produce mCol17 in transplanted $COL17^{m-/-}$ mice. (*A*) HSCs and MSCs from GFP+ Tg mice were sorted or cultured. One or the other type of these stem cells with supporting $COL17^{m-/-}$ whole BM cells were injected into preirradiated $COL17^{m-/-}$ mice. (*B*) Sparse GFP+ cytokeratin+ cells, shown by white arrows, are detected in the epithelized skin of HSC-BMT model mouse (*Upper*). Also in the MSC-BMT model, GFP+ cytokeratin+ cells are observed (*Lower*). (Scale bars: 10 μm.) (*C*) Punctate staining of mCol17 is noted, shown as yellow arrows, in the epithelized skin tissue of both HSC- and MSC-BMT model mice. (Scale bars: 20 μm.) (*D*) RT-PCR analysis of the epithelized skin area after full-thickness wounding. Both HSCs (lane 1) and MSCs (lane 2) in the BMT treatment model express positive *mCol17*. Also, single i.v. injection of GFP+ MSCs (lane 3) induces weak *mCol17* mRNA expression. (*E*) At 90 d after treatment, the HSC-BMT model mice (*Center*) demonstrate better clinical manifestations than the untreated $COL17^{m-/-}$ mice (*Left*), whereas mice of the MSC-BMT models (*Right*) tend to show more severe perianal erosions and hair loss.

lamina and dermis. Recently, various treatments were reported to restore the deficient proteins. These approaches fall mainly into three strategies: gene therapy (20–24), protein therapy (21, 25, 26), and cell therapy. Cell therapies using fibroblasts have been attempted for recessive dystrophic EB (RDEB) model mice and human patients, both of which lack collagen VII. Intradermal fibroblast cell therapy was reported for RDEB model mice (18) and RDEB human patients (27). These approaches may prove to be fundamental treatments for EB. However, their effects are transient and occur only where the genes, proteins, or cells are introduced; they may cause rejection and such gene-correction approaches still raise questions of ethics and safety. Woodley et al. (28) recently reported that i.v. injection of human fibroblasts induces systemic production of human collagen VII in immunodeficient mice; however, major ethical and safety problems remain in human patients.

BMT, an established, widely used medical technique for hematologic malignancies, has recently been attempted for severe hereditary genetic disorders. Hobbs et al. (29) first reported the

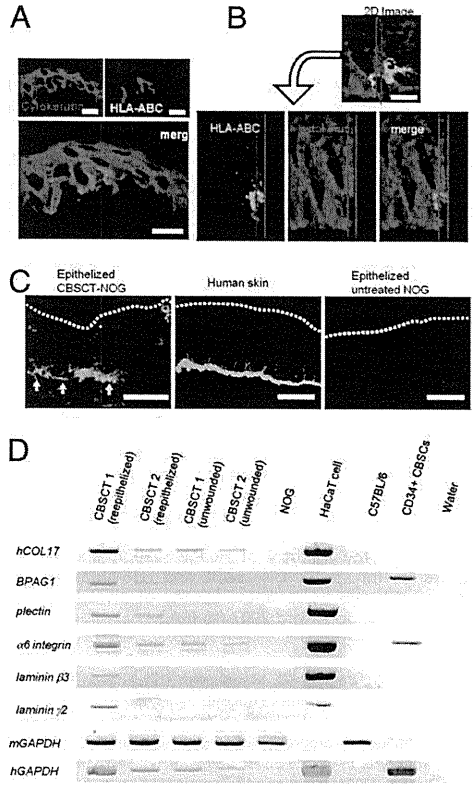

Fig. 5. Human hematopoietic stem cell transplantation induces human epidermal keratinocytes that produce BMZ proteins. (*A*) The epithelized skin samples of treated NOG mice include sporadic cytokeratin$^+$ (red), HLA-ABC$^+$ (blue) cells in the basal cell layer, which indicate human cord blood-derived keratinocytes. (Scale bars: 10 μm.) (*B*) 3D analyses of the immunohistochemical sections prove costaining of keratin (red) and HLA-ABC (green), indicating that these cells are human cord blood-derived keratinocytes and not two distinct overlaid cells. Blue lines: cross-section edges. (Scale bar: 10 μm.) (*C*) Sparse, linear deposition of hCOL17 is noted in the epithelized skin of CBSCT-treated NOG mice (yellow arrows). Green: hCOL17 (D20); red: cytokeratin; (Scale bars: 20 μm.) (*D*) RT-PCR analysis for two transplanted NOG mice, for both unwounded and epithelized skin (CBSCT 1 and CBSCT 2). The expression of several BMZ proteins, *hCOL17, BPAG1, plectin, α6 integrin, laminin β3,* and *laminin γ2* mRNA is demonstrated. Unwounded skin shows faint expression of *hCOL17* and *α6 integrin*.

efficacy of BMT for treatment of Hurler's syndrome. Later hematopoietic stem cell transplantation proved effective in other mucopolysaccharidoses (30–33). More recently, Sampaolesi et al. (34) reported on the potential of stem cell therapy for the treatment of Duchene muscular dystrophy. These experiments indicate that stem cell therapies including BMT are promising candidates for several congenital genetic disorders. BMT techniques have three advantages over previous cell therapies: (*i*) systemic and long-lasting effects can be expected from the circulating BM-derived cells, (*ii*) conventional BMT techniques can be used in clinical applications, and therefore (*iii*) fewer ethical problems arise from the treatment.

Recently Tolar et al. (35) reported that hematopoietic stem cells contributed to life prolongation in RDEB neonatal mice. Chino et al. (36) reported that treatment of embryonic BMT in RDEB mice induced the expression of donor-derived fibroblasts and type VII collagen. These reports investigated neonatal or embryonic mice and focused on type VII collagen, which is produced mainly by dermal fibroblasts. In this study we show the potential of BMT therapies in adult mice with cutaneous congenital disorders caused by deficiencies of transmembrane proteins such as COL17, which is produced mainly by keratinocytes.

As to the origin of the BM-derived cells that differentiated into epidermal cells, Tolar et al. reported that only CD150$^+$ CD48$^-$ HSCs contributed to the amelioration of RDEB mice; nevertheless, MSCs abundantly expressed type VII collagen mRNA (35). Conversely, we and other groups have reported that MSCs also have the potential to differentiate into keratinocytes (37, 38). Our experiments have shown that both HSCs and MSCs have the potential to produce Col17. However, a BMT model with infusion of enriched MSCs tended to induce more severe clinical manifestations. One hypothesis is that the infused MSCs in BMT reside so shortly that long-term effects, such as clinical improvement, might not occur (39, 40). We demonstrated that human cord blood CD34$^+$ HSCs are able to differentiate into keratinocytes in vivo. Although further investigation is needed, we suggest that the difference between the benefits of MSC and HSC transplantations owes to the lack of a long-term, renewable circulating source of Col17-producing cells induced by donor hematopoiesis. From these findings we conclude that both HSCs and MSCs contributed to the production of Col17, although HSCs played more a significant role in clinical improvement in our EB model mice.

Recently Kopp et al. (41) performed BMT and subsequent skin transplantation in one Herlitz-junctional EB infant but unfortunately the child died. They performed normal conditioning treatments similar to those used in hematological malignancies, but the treatments might be too strong for EB patients. Indeed, in our EB model mice, we had to reduce the irradiation dose before BMT to avoid erosions. This report is highly suggestive toward determining conditioning regimens.

In conclusion, we confirmed the reexpression of the previously deficient anchoring protein Col17, better clinical appearance, and longer life expectancy after BMT in our junctional EB model mice. Furthermore we demonstrated that human HSCs can contribute to the regeneration of wounded skin, producing structural proteins in the BMZ. Current conventional hematopoietic stem cell transplantation will lead to treatments for severe forms of EB or even other congenital skin disorders involving epidermal structural proteins.

Materials and Methods

Bone Marrow Transplantation. Recipient adult mice were irradiated with a lethal dose of X-rays at 9 Gy (C57BL/6 and *COL17*$^{m-/-,h+}$ mice) or 6 Gy (in *COL17*$^{m-/-}$ mice), 12 h before infusions. The 9-Gy irradiation resulted in severe erosions and hair loss within 4 wk after BMT to *COL17*$^{m-/-}$ mice. Approximately 3.0–6.0 × 10^6 murine BM-derived cells in 400 μL PBS were injected through the mouse tail vein.

Human Cord Blood Stem Cell Transplantation. Recipient adult NOG mice were irradiated with a sublethal dose of X-rays at 2.5 Gy. Twelve hours later, approximately 1.0–2.5 × 10^5 human CD34$^+$ cells in 400 μL PBS were injected through the mouse tail vein. Hematopoietic reconstitution was evaluated in peripheral blood mononuclear cells 12 wk after transplantation.

Hematopoietic and Mesenchymal Cell Transplantations. Recipient adult *COL17*$^{m-/-}$ mice were irradiated with a lethal dose of X-rays at 6 Gy. Twelve hours later, approximately 5.0 × 10^3 GFP$^+$ HSCs (n = 5) or 5.0 × 10^5 GFP$^+$ MSCs (n = 4) were mixed with 5.0 × 10^5 whole *COL17*$^{m-/-}$ BM-derived cells in 400 μL PBS and injected through the mouse tail vein.

RT-PCR Analyses. For RT-PCR, total RNA from tissues and cells was extracted using Isogen (Nippon Gene) and 200 ng of total RNA was used for cDNA synthesis in SuperScript II reverse transcriptase according to the manufacturer's instructions (Invitrogen). RT-PCR analysis of mRNA was performed in a thermocycler (GeneAmp PCR system 9600; Perkin-Elmer). The primers specific for protein sequences are summarized in Table S1. The PCR protocol for these genes included 35 cycles of amplification (denaturing at 94 °C for 1 min, annealing for 1 min, elongation at 72 °C for 1 min). Aliquots from each amplification reaction were analyzed by electrophoresis in 2% acrylamide-Tris-borate gels. Gel images were acquired and processed by an image analyzer (LAS-4000UVmini; Fujifilm).

Western Blotting. Protein lysates from epidermal tissues were subjected to SDS/PAGE and electrophoretically transferred onto a nitrocellulose membrane. The membranes were blocked with 1% nonfat dry milk in PBS, probed with rat monoclonal antibodies against mCol17 (KT4.2, 1:80,000), and then allowed to react with goat anti-rat IgG antibody coupled with HRP (1:1,000; Southern Biotech). For loading control, we used mouse anti-β-actin antibody

(1:1,000; Sigma-Aldrich) and HRP-conjugated goat anti-mouse IgG (1:1,000; Southern Biotech). The resultant immune complexes were visualized using a chemiluminescent detection system (LumiGLO; Cell Signaling Technology) and processed by an image analyzer (LAS-4000UVmini).

Ultrastructural Observations. Skin biopsy samples of two mice each from GFP^+ Tg mice, untreated $COL17^{m-/-}$ mice, and BMT-treated $COL17^{m-/-}$ mice were fixed in 5% glutaraldehyde solution, postfixed in 1% osmium tetroxide, dehydrated, and embedded in Epon 812. The samples were sectioned at 1-μm thickness for light microscopy and thin-sectioned at 70-nm thickness for electron microscopy. The thin sections were stained with uranyl acetate and lead citrate and examined under a transmission electron microscope (H-7100; Hitachi High-Technologies).

Clinical Evaluation of $COL17^{m-/-}$ Mice. After bone marrow transplantation, the clinical severity of the BMT-treated $COL17^{m-/-}$ mice, such as spontaneous erosions and blistering, was evaluated and compared with that of the untreated $COL17^{m-/-}$ mice and BMT-control mice whose donors were $COL17^{m-/-}$ mice. The perioral area and circumanal area tend to be naturally predisposed to erosion. We investigated the clinical severity by measuring the share of each affected area as a percent of its entire region. These were assessed by two independent assessors viewing the same clinical images. In addition we compared the vital prognosis after BMT (35 d after birth) among BMT-treated mice (n = 20), untreated $COL17^{m-/-}$ mice (n = 17), and BMT-control mice (n = 6).

Mechanical Rubber Stress Test. The epithelized dorsal skin areas of 1 cm^2 after erosion were marked with a pen and exposed to a mechanical rubber stress test as previously reported (18). The skin was gently stretched, and mechanical shearing forces were applied by the same investigator repeatedly (25 times) as intense, unidirectional rubbing with a pencil eraser. After 20 min, skin specimens were excised and processed for histopathological analysis. Also, we measured the total areas of erosion by ImageJ software (42).

Statistical Analyses. Mann–Whitney U test for nonparametric data, Kaplan-Meier analysis for survival curves, and log-rank test for survival evaluation were performed using Excel 2003 (Microsoft) with the add-in software Statcel2 (OMS) (43). For comparison of more than two groups, data were analyzed by Kruskal–Wallis test followed by Scheffe's F test. Results were expressed as mean ± SE.

ACKNOWLEDGMENTS. We thank Prof. K. B. Yancey (Department of Dermatology, Medical College of Wisconsin, Milwaukee, WI) for providing the $COL17^{m+/+,h+}$ mice, Prof. K. Owaribe (Division of Biological Science, Graduate School of Science, Nagoya University, Nagoya, Japan) for the gift of antibodies against human COL17 (D20), and Prof. T. Tanaka (Department of Dermatology, Shiga University of Medical Science, Otsu, Japan) for the gift of antibodies against mouse Col17 (KT4.2). This work was supported in part by grants-in-aid for scientific research (13357008 and 17209038 to H.S. and 15790563 to R.A.) and the Project for Realization of Regenerative Medicine (H.S.) from the Ministry of Education, Science, Sports, and Culture of Japan; by the program for Promotion of Fundamental Studies in Health Sciences of the National Institute of Biomedical Innovation (06-42 to H.S.); by Health and Labor Sciences Research Grants from the Ministry of Health, Labor, and Welfare of Japan (H13-Measures for Intractable Disease-02 and H16-Measures for Intractable Disease-02, to H.S.); and by Japanese Society of Investigative Dermatology (JSID) Fellowship Shiseido Award 2007 (to R.A.).

1. Satake K, Lou J, Lenke LG (2004) Migration of mesenchymal stem cells through cerebrospinal fluid into injured spinal cord tissue. *Spine (Phila Pa 1976)* 29:1971–1979.
2. Herzog EL, Chai L, Krause DS (2003) Plasticity of marrow-derived stem cells. *Blood* 102: 3483–3493.
3. Jiang Y, et al. (2002) Pluripotency of mesenchymal stem cells derived from adult marrow. *Nature* 418:41–49.
4. Orlic D, et al. (2001) Bone marrow cells regenerate infarcted myocardium. *Nature* 410: 701–705.
5. Kocher AA, et al. (2001) Neovascularization of ischemic myocardium by human bone-marrow-derived angioblasts prevents cardiomyocyte apoptosis, reduces remodeling and improves cardiac function. *Nat Med* 7:430–436.
6. Ferrari G, et al. (1998) Muscle regeneration by bone marrow-derived myogenic progenitors. *Science* 279:1528–1530.
7. Yamada M, et al. (2004) Bone marrow-derived progenitor cells are important for lung repair after lipopolysaccharide-induced lung injury. *J Immunol* 172:1266–1272.
8. Kale S, et al. (2003) Bone marrow stem cells contribute to repair of the ischemically injured renal tubule. *J Clin Invest* 112:42–49.
9. Wagers AJ, Sherwood RI, Christensen JL, Weissman IL (2002) Little evidence for developmental plasticity of adult hematopoietic stem cells. *Science* 297:2256–2259.
10. Lagasse E, et al. (2000) Purified hematopoietic stem cells can differentiate into hepatocytes in vivo. *Nat Med* 6:1229–1234.
11. Fine JD, et al. (2008) The classification of inherited epidermolysis bullosa (EB): Report of the Third International Consensus Meeting on Diagnosis and Classification of EB. *J Am Acad Dermatol* 58:931–950.
12. Mavilio F, et al. (2006) Correction of junctional epidermolysis bullosa by transplantation of genetically modified epidermal stem cells. *Nat Med* 12:1397–1402.
13. Banasik MB, McCray PB, Jr (2010) Integrase-defective lentiviral vectors: Progress and applications. *Gene Ther* 17:150–157.
14. Murata H, et al. (2007) Donor-derived cells and human graft-versus-host disease of the skin. *Blood* 109:2663–2665.
15. Harris RG, et al. (2004) Lack of a fusion requirement for development of bone marrow-derived epithelia. *Science* 305:90–93.
16. Inokuma D, et al. (2006) CTACK/CCL27 accelerates skin regeneration via accumulation of bone marrow-derived keratinocytes. *Stem Cells* 24:2810–2816.
17. Nishie W, et al. (2007) Humanization of autoantigen. *Nat Med* 13:378–383.
18. Fritsch A, et al. (2008) A hypomorphic mouse model of dystrophic epidermolysis bullosa reveals mechanisms of disease and response to fibroblast therapy. *J Clin Invest* 118:1669–1679.
19. Ito M, et al. (2002) NOD/SCID/gamma(c)(null) mouse: An excellent recipient mouse model for engraftment of human cells. *Blood* 100:3175–3182.
20. Bauer JW, Lanschuetzer C (2003) Type XVII collagen gene mutations in junctional epidermolysis bullosa and prospects for gene therapy. *Clin Exp Dermatol* 28:53–60.
21. Robbins PB, Sheu SM, Goodnough JB, Khavari PA (2001) Impact of laminin 5 beta3 gene versus protein replacement on gene expression patterns in junctional epidermolysis bullosa. *Hum Gene Ther* 12:1443–1448.
22. Robbins PB, et al. (2001) In vivo restoration of laminin 5 beta 3 expression and function in junctional epidermolysis bullosa. *Proc Natl Acad Sci USA* 98:5193–5198.
23. Dellambra E, et al. (2001) Gene correction of integrin beta4-dependent pyloric atresia-junctional epidermolysis bullosa keratinocytes establishes a role for beta4 tyrosines 1422 and 1440 in hemidesmosome assembly. *J Biol Chem* 276:41336–41342.
24. Seitz CS, Giudice GJ, Balding SD, Marinkovich MP, Khavari PA (1999) BP180 gene delivery in junctional epidermolysis bullosa. *Gene Ther* 6:42–47.
25. Igoucheva O, Kelly A, Uitto J, Alexeev V (2008) Protein therapeutics for junctional epidermolysis bullosa: Incorporation of recombinant beta3 chain into laminin 332 in beta3-/- keratinocytes in vitro. *J Invest Dermatol* 128:1476–1486.
26. Woodley DT, et al. (2004) Injection of recombinant human type VII collagen restores collagen function in dystrophic epidermolysis bullosa. *Nat Med* 10:693–695.
27. Wong T, et al. (2008) Potential of fibroblast cell therapy for recessive dystrophic epidermolysis bullosa. *J Invest Dermatol* 128:2179–2189.
28. Woodley DT, et al. (2007) Intravenously injected human fibroblasts home to skin wounds, deliver type VII collagen, and promote wound healing. *Mol Ther* 15:628–635.
29. Hobbs JR, et al. (1981) Reversal of clinical features of Hurler's disease and biochemical improvement after treatment by bone-marrow transplantation. *Lancet* 2:709–712.
30. Sands MS, et al. (1997) Murine mucopolysaccharidosis type VII: Long term therapeutic effects of enzyme replacement and enzyme replacement followed by bone marrow transplantation. *J Clin Invest* 99:1596–1605.
31. Warkentin PI, Dixon MS, Jr, Schafer I, Strandjord SE, Coccia PF (1986) Bone marrow transplantation in Hunter syndrome: A preliminary report. *Birth Defects Orig Artic Ser* 22:31–39.
32. Krivit W, et al. (1984) Bone-marrow transplantation in the Maroteaux-Lamy syndrome (mucopolysaccharidosis type VI). Biochemical and clinical status 24 months after transplantation. *N Engl J Med* 311:1606–1611.
33. Gasper PW, et al. (1984) Correction of feline arylsulphatase B deficiency (mucopolysaccharidosis VI) by bone marrow transplantation. *Nature* 312:467–469.
34. Sampaolesi M, et al. (2006) Mesoangioblast stem cells ameliorate muscle function in dystrophic dogs. *Nature* 444:574–579.
35. Tolar J, et al. (2009) Amelioration of epidermolysis bullosa by transfer of wild-type bone marrow cells. *Blood* 113:1167–1174.
36. Chino T, et al. (2008) Bone marrow cell transfer into fetal circulation can ameliorate genetic skin diseases by providing fibroblasts to the skin and inducing immune tolerance. *Am J Pathol* 173:803–814.
37. Wu Y, Chen L, Scott PG, Tredget EE (2007) Mesenchymal stem cells enhance wound healing through differentiation and angiogenesis. *Stem Cells* 25:2648–2659.
38. Sasaki M, et al. (2008) Mesenchymal stem cells are recruited into wounded skin and contribute to wound repair by transdifferentiation into multiple skin cell type. *J Immunol* 180:2581–2587.
39. Rieger K, et al. (2005) Mesenchymal stem cells remain of host origin even a long time after allogeneic peripheral blood stem cell or bone marrow transplantation. *Exp Hematol* 33:605–611.
40. Dickhut A, et al. (2005) Mesenchymal stem cells obtained after bone marrow transplantation or peripheral blood stem cell transplantation originate from host tissue. *Ann Hematol* 84:722–727.
41. Kopp J, et al. (2005) Hematopoietic stem cell transplantation and subsequent 80% skin exchange by grafts from the same donor in a patient with Herlitz disease. *Transplantation* 79:255–256.
42. Abramoff MD, Magelhaes PJ, Ram SJ (2004) Image Processing with ImageJ. *Biophotonics International* 11:36–42.
43. Yanai H (2004) *Statcel-The Useful Add-In Software Forms on Excel* (OMS, Tokyo) 2nd Ed.

Corrections and Retraction

CORRECTIONS

GENETICS

Correction for "Lack of association of common variants on chromosome 2p with primary open-angle glaucoma in the Japanese population," by Fumihiko Mabuchi, Yoichi Sakurada, Kenji Kashiwagi, Zentaro Yamagata, Hiroyuki lijima, and Shigeo Tsukahara, which appeared in issue 21, May 25, 2010, of *Proc Natl Acad Sci USA* (107:E90–E91; first published April 27, 2010; 10.1073/pnas.0914903107).

The authors note that, due to a printer's error, the author name Hiroyuki lijima should have appeared as Hiroyuki Iijima. The corrected author line appears below. The online version has been corrected.

Fumihiko Mabuchi[a,1], Yoichi Sakurada[a], Kenji Kashiwagi[a], Zentaro Yamagata[b], Hiroyuki Iijima[a], and Shigeo Tsukahara[a]

www.pnas.org/cgi/doi/10.1073/pnas.1008743107

MEDICAL SCIENCES

Correction for "Bone marrow transplantation restores epidermal basement membrane protein expression and rescues epidermolysis bullosa model mice," by Yasuyuki Fujita, Riichiro Abe, Daisuke Inokuma, Mikako Sasaki, Daichi Hoshina, Ken Natsuga, Wataru Nishie, James R. McMillan, Hideki Nakamura, Tadamichi Shimizu, Masashi Akiyama, Daisuke Sawamura, and Hiroshi Shimizu, which appeared in issue 32, August 10, 2010, of *Proc Natl Acad Sci USA* (107:14345–14350; first published July 26, 2010; 10.1073/pnas.1000044107).

The authors note that, due to a printer's error, Yasuyuki Fujita was omitted as the first author of this article. The corrected author line appears below. The online and print versions have been corrected.

Yasuyuki Fujita[a], Riichiro Abe[a,1], Daisuke Inokuma[a], Mikako Sasaki[a], Daichi Hoshina[a], Ken Natsuga[a], Wataru Nishie[a], James R. McMillan[a], Hideki Nakamura[a], Tadamichi Shimizu[b], Masashi Akiyama[a], Daisuke Sawamura[c], and Hiroshi Shimizu[a,1]

www.pnas.org/cgi/doi/10.1073/pnas.1011158107

RETRACTION

MEDICAL SCIENCES

Retraction for "Complete and persistent phenotypic correction of phenylketonuria in mice by site-specific genome integration of murine phenylalanine hydroxylase cDNA," by Li Chen and Savio L. C. Woo, which appeared in issue 43, October 25, 2005, of *Proc Natl Acad Sci USA* (102:15581–15586; first published October 17, 2005; 10.1073/pnas.0503877102).

The undersigned author wishes to note the following: "After re-examining the laboratory records, I have concluded that there are data irregularities underlying this paper that warrant its retraction. I regret not recognizing these irregularities before the manuscript was published and apologize for any inconvenience this might have caused."

Savio L. C. Woo

www.pnas.org/cgi/doi/10.1073/pnas.1009071107

Diagnostic Pitfalls of Using Dermoscopic Features to Differentiate Between Malignant Melanoma and Pigmented Seborrhoeic Keratosis

Satoru Aoyagi, Hiroo Hata, Kentaro Izumi, Maria Maroto Iitani and Hiroshi Shimizu
Department of Dermatology, Hokkaido University Graduate School of Medicine, N15 W7, Kita-ku, Sapporo 060-8638, Japan. E-mail: saoyagi@med.hokudai.ac.jp
Accepted March 3, 2010.

Differentiation of malignant melanomas (MM) and the pigmented variant of seborrhoeic keratosis (SK) can be difficult. Cases of MM mimicking SK (1) and of SK clinically mimicking MM (2) have been reported. Dermoscopy is a useful non-invasive method of differential diagnosis between MM and SK. However, these tumours have several histological variants whose specific dermoscopic findings are not always the same (3). We report here a case of pigmented SK on the lower leg that clinically mimicked MM. We describe the pitfalls of using dermoscopic features for differential diagnosis, with reference to this case.

CASE REPORT

An 80-year-old Japanese man was referred to our department for the treatment of a pigmented lesion on the lower leg. The lesion had been gradually enlarging for 6 months. Physical examination revealed a black nodule 2 cm in diameter, with a light-brownish pigmented macule with a long axis of 3.5 cm at the base of the nodule (Fig. 1). Dermoscopic examination showed a pigmented network-like structure in the area of the macule (Fig. 2a) where prominent multi-component structure in the area of the nodule. Irregular black globules and a conspicuous blue-whitish veil predominated (Fig. 2b). Comedo-like openings were not detectable and faint milia-like cysts were seen, although the blue-whitish veil made them difficult to recognize. Histological examination by excision showed the intraepidermal proliferation of highly pigmented basaloid cells intermingled with horn cysts corresponding to typical SK.

Fig. 1. A blackish nodule arising from a reticular dark-brownish pigmented macule appears on the lower leg. Dermoscopic finding is shown in Fig. 2. Excision showed seborrhoeic keratosis.

DISCUSSION

Regarding the first decision on differentiation by dermoscopic diagnosis of the pigmented tumours, the most important point is to avoid misdiagnosing SK as melanocytic tumour. If the lesion is considered melanocytic, it might lead to the diagnosis of MM in many cases (4). It is reported that pigmented SK sometimes shows a network structure that resembles the pigmented network seen in melanocytic lesions. Conversely, the most common dermoscopic characteristics of SK are a comedo-like opening and milia-like cysts. However, the specificity of these findings is not 100% (5) and in some cases the area of comedo-like opening is undetectable as such against the background of diffuse, brown homogeneous pigmentation.

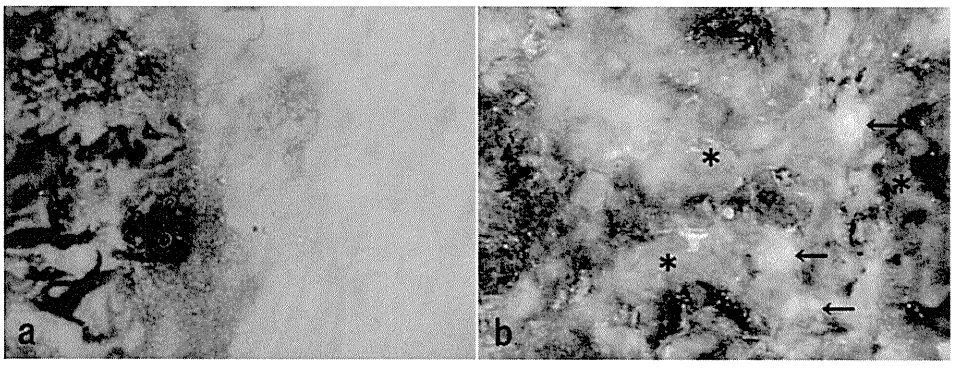

Fig. 2. a) The pseudo-pigment network in the area of the macule. b) Irregular black globules and a conspicuous blue-whitish veil (*asterisk*) predominate in the nodule. Meticulous observation reveals milia-like cysts (*arrows*) within the blue-whitish veil.

In our case, the most common dermoscopic findings of SK (comedo-like openings and milia-like cysts) were not clearly visible. For practitioners who have little experience with pigmented SK, it is easy to mistake pigmented SK for MM, which often shows a multi-component structure with a pseudo-network.

To improve the reliability of dermoscopic differential diagnosis between pigmented SK and MM, we highlight 3 diagnostic pitfalls based on our case: (*i*) misdiagnosing a pseudo-network as an atypical pigment network, (*ii*) making errors in perception such as mistaking multi-component structure with a pseudo-network for malignant findings, and (*iii*) failing to make meticulous observation to detect insignificant milia-like cysts. Careful evaluation of the entire lesion must be undertaken to ensure that the dermoscopic findings are all consistent with the diagnosis.

The authors declare no conflict of interest.

REFERENCES

1. Braga JC, Scope A, Klaz I, Mecca P, Spencer P, Marghoob AA. Melanoma mimicking seborrheic keratosis: an error of perception precluding correct dermoscopic diagnosis. J Am Acad Dermatol 2008; 58: 875–880.
2. de Giorgi V, Massi D, Salvini C, Mannone F, Carli P. Pigmented seborrheic keratoses of the vulva clinically mimicking a malignant melanoma: a clinical, dermoscopic-pathologic case study. Clin Exp Dermatol 2005; 30: 17–19.
3. Carrera C, Segura S, Palou J, Puig S, Segura J, Martí RM, et al. Seborrheic keratosislike melanoma with folliculotropism. Arch Dermatol 2007; 143: 373–376.
4. Braun RP, Rabinovitz HS, Krischer J, Kreusch J, Oliviero M, Naldi L, et al. Dermoscopy of pigmented seborrheic keratosis: a morphological study. Arch Dermatol 2002; 138: 1556–1560.
5. Elgart GW. Seborrheic keratoses, solar lentigines, and lichenoid keratoses. Dermatoscopic features and correlation to histology and clinical signs. Dermatol Clin 2001; 19: 347–357.

Journal of Surgical Oncology 2010;101:175–179

HOW I DO IT

Controlling the Histological Margin for Non-Melanoma Skin Cancer Conveniently Using a Double-Bladed Scalpel

SATORU AOYAGI, MD, PhD,* HIROO HATA, MD, ERINA HOMMA, MD, AND HIROSHI SHIMIZU, MD, PhD
Department of Dermatology, Hokkaido University Graduate School of Medicine, Sapporo, Japan

Background: In some countries, intraoperative histological evaluation to control the surgical margin for non-melanoma skin cancer is widely used instead of Mohs micrographic surgery. Nevertheless, this evaluation by frozen section analysis is usually limited to suspicious areas.
Objectives: To evaluate the efficacy of double-bladed scalpel for intraoperative histological margin control for non-melanoma skin cancers.
Methods: Between 2005 and 2009, 10 basal cell carcinomas and 5 squamous cell carcinomas were underwent complete histological margin control in which a double-bladed scalpel was used during the surgery at the Hokkaido University Hospital in Japan.
Results: The mean number of re-excisions required for complete tumor resection was 1.4 times. Nine (60%) of the 15 patients obtained histological clearance of all surgical margins at the first re-excision. The mean size of total surgical margin was 6.1 mm (range: 2–12 mm). The median time from the first tumor excision to reconstruction was 124 min. No local recurrences have been reported.
Conclusions: This method may be used as an alternative for complete histological margin control at many hospitals where it is difficult to perform Mohs micrographic surgery.
J. Surg. Oncol. 2010;101:175–179. © 2010 Wiley-Liss, Inc.

KEY WORDS: **basal cell carcinoma; squamous cell carcinoma; Mohs micrographic surgery; intraoperative histological evaluation; frozen section**

INTRODUCTION

Non-melanoma skin cancer (NMSC) is the most common malignancy in the world, and its incidence continues to rise [1]. The majority of these are basal cell carcinomas (BCCs) and squamous cell carcinomas (SCCs). Standard excision with adequate surgical margin is the most common surgical treatment for these, providing a high cure rate for small, low-risk skin cancers [2]. In conventional surgery, where the samples are sent to pathology for margin assessment, the tissues are sliced vertically at 2- to 4-mm intervals to make microscopic sections.

Some of these cancers that grow asymmetrically and with a much wider subclinical extension tend to show high recurrence rates [3,4]. For these high-risk continuous skin cancers, Mohs micrographic surgery (MMS), which is based on the concept of excising skin cancer layer by layer and examining horizontally cut specimen sections, affords a high cure rate by achieving precise removal [5]. MMS is a well-established technique; it is the gold standard of care for selected cases of skin cancers in Western countries [5].

However, due to differences among countries in insurance systems and surgical approaches, MMS is still uncommon in Asian countries [6]. In some communities, intraoperative histological evaluation to control the surgical margin is widely used instead of MMS [7]. Nevertheless, intraoperative histological evaluation by frozen section analysis is usually limited to suspicious areas. The accuracy of such analysis for detecting hisitological surgical margin of skin cancer is highly dependent on the methods used to obtain and analyze the margins. For institutions at which it is difficult to perform MMS, we introduce double-bladed scalpel (DBS) as a novel simple method for complete histological margin control (Fig. 1). This improves the pathodiagnostic reliability of conventional intraoperative histological evaluation.

MATERIALS AND METHODS

Between September 2005 and August 2009, 15 patients with biopsy-proven BCC or SCC were referred to our institution for treatment of their lesion and underwent complete histological margin control in which a DBS was used during the surgery at the Department of Dermatology, Hokkaido University Hospital in Japan. The indications for this procedure were histologically aggressive subtype (BCC: morpheaform, infiltrative, micronodular; SCC: poorly differentiated), high risk of recurrence (BCC on the H-zone of the face; SCC on the lip and ear) and tumor with ill-defined clinical margins. Information recorded included the patient age and gender, the lesion site and clinical features, the tumor size, the histological diagnosis and subtype, the type of anesthesia, the total time required for the procedure, the type of reconstruction, the number of re-excisions required to achieve tumor-free margins, the initial and final surgical margin, and the outcome.

Prior to surgery, the gross macroscopic extent of the tumor was measured as the long axis and recorded as the tumor size. Each margin after re-excision was added to the initial surgical margin. After surgery had achieved a histologically negative margin, the measurement of this margin was recorded as the final surgical margin. The clinical

*Correspondence to: Satoru Aoyagi, MD, PhD, Department of Dermatology, Hokkaido University Graduate School of Medicine, N15 W7, Kita-ku, Sapporo 060-8638, Japan. Fax: +81-11-706-7820.
E-mail: saoyagi@med.hokudai.ac.jp

Received 30 September 2009; Accepted 20 October 2009
DOI 10.1002/jso.21456
Published online in Wiley InterScience (www.interscience.wiley.com).

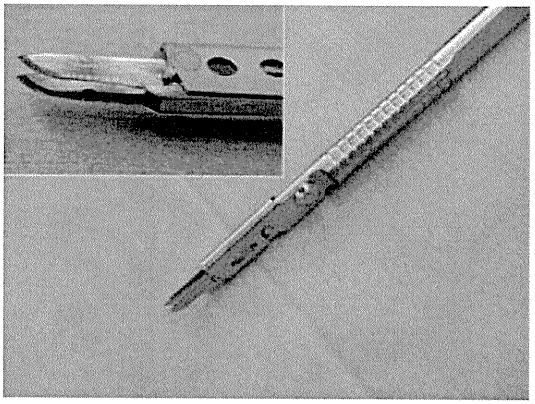

Fig. 1. A newly devised DBS set with a 2-mm interblade gap with a lightweight cylindrical holder.

and histological features of the patients are shown in Table I. This procedure is detailed in Figure 2.

Surgical Technique

Before injection of local anesthesia, the gross tumor and surgical margins were marked with blue ink under meticulous dermoscopic observation. Initial surgical margins of 2–5 mm were proposed, with the size depending on the condition of the patient. The adequate margin will vary with tumor size, location, clinical definition of border and surgeon's preference. Next, using a DBS, the inside blade was set at the surgical margin line and an excision was made at least to the depth of the subcutaneous tissue (Fig. 2A). Then two parallel lines were made to excise a 2-mm width around the tumor.

The gross tumor with initial surgical margin was then excised in a bowl shape (Fig. 2B) and sent to the pathology lab for conventional paraffin-embedded vertical sections, for assessment a few days after the surgery.

After excision of the tumor, the defect was sub-sectioned into two to four regions (Fig. 2C). The sub-sectioned defect was excised along with the outer 2-mm strips of skin made by DBS. It was excised at a uniform width by scissors with great care to avoid tearing tissue (Fig. 2D), as in re-excision of an additional layer for histological analysis in conventional MMS.

The re-excised specimens were flattened and face down from the tumor side for the preparation of a frozen tissue block of specimen. Horizontal sections were sliced starting from the true margin side. Sections were stained in the conventional manner with hematoxylin and eosin. The horizontal sectioning of the re-excised tissue layer allows for the identification of both deep and peripheral margins on the same section. This is an important essential technique of MMS in our method, as the complete surgical margin can be evaluated histologically.

All slides were examined by a dermatologic surgeon and pathologist together during the surgery. If a tumor-positive margin in a re-excision specimen was obtained, additional layers of tissue were excised from the tumor-positive area. This second excision specimen was sent for permanent-section analysis a few days after the surgery. Defect repair was performed by a dermatologic surgeon on the same day, except when a tumor-positive margin was obtained in re-excision. When any of the additional layers of the margins ware positive, the reconstruction was scheduled for the postoperative day after tumor-free margins were confirmed by conventional margin assessment in permanent slides.

RESULTS

All 15 of the primary tumors (10 BCCs and 5 SCCs) from 15 patients were completely resected with complete histological margin control using DBS during the surgery. These tumors were also histologically confirmed by permanent section later. The 15 patients (8 male (53.3%), 7 female (46.7%)) met the criteria of histologically aggressive subtype, high risk of recurrence and tumor with ill-defined clinical margins. The median age was 72.6 years (range: 48–90). All patients were ethnic Japanese. All tumors were located on the head and neck, with five (33.3%) on the nose, five (33.3%) on the lip, two (13.3%) on the cheek, one (6.7%) on the cantus, one on the neck and one on the ear. The median size of tumor was 18.5 mm (Table 1).

Four (26.7%) of the 15 patients had the surgery under general anesthesia. The mean number of re-excisions required for complete tumor resection was 1.4 times. Nine (60%) of the 15 patients obtained histological clearance of all surgical margins at the first re-excision. Six patients (40%) required an additional re-excisional layer to achieve clear margins. The mean size of initial surgical margin was 4.6 mm (range: 2–10 mm) and the total surgical margin was 6.1 mm (range: 2–12 mm). Surgical defects were reconstructed with primary closure in 2 patients (13.3%), local flap in 9 patients (60%), and combination of local flap and tissue grafting in 4 patients (26.7%). The median time

TABLE I. Summary of Clinical Histological Features of NMSC Cases in the Present Study

Case	Age/gender	Diagnosis	Tumor site	Tumor size (mm)	Clinical feature of the lesion	Histologic subtype
1	81/F	BCC	Cantus	8	Ill-demarcated, pink colored plaque	Micronodular
2	87/M	BCC	Lip	14	Ill-demarcated, pink colored nodule	Micronodular
3	75/M	BCC	Neck	32	Well-demarcated, slightly pigmented, ulcerated nodule	Micronodular
4	64/F	BCC	Cheek	10	Ill-demarcated, pink colored nodule	Micronodular
5	77/F	BCC	Cheek	11	Ill-Demarcated, pink colored nodule	Micronodular
6	77/M	BCC	Ear	8	Ill-demarcated, slightly pigmented, ulcerated plaque	Morpheic
7	69/F	BCC	Nose	7	Ill-demarcated, red colored plaque	Morpheic
8	68/M	BCC	Nose	11	Well-demarcated, slightly pigmented nodule	Micronodular
9	71/F	BCC	Nose	25	Ill-demarcated, pink colored, ulcerated nodule	Morpheic
10	56/M	BCC	Nose	30	Ill-demarcated, slightly pigmented, ulcerated plaque	Morpheic
11	82/F	SCC	Nose	20	Well-demarcated, red colored, ulcerated nodule	Poorly differentiated
12	90/M	SCC	Lip	20	Well-demarcated, pink colored, keratotic nodule	Moderately differentiated
13	48/M	SCC	Lip	32	Ill-demarcated, red colored, keratotic nodule	Poorly differentiated
14	65/M	SCC	Lip	10	Well-demarcated, pink colored, ulcerated nodule	Moderately differentiated
15	79/F	SCC	Lip	40	Ill-demarcated, red colored, ulcerated nodule	Moderately differentiated

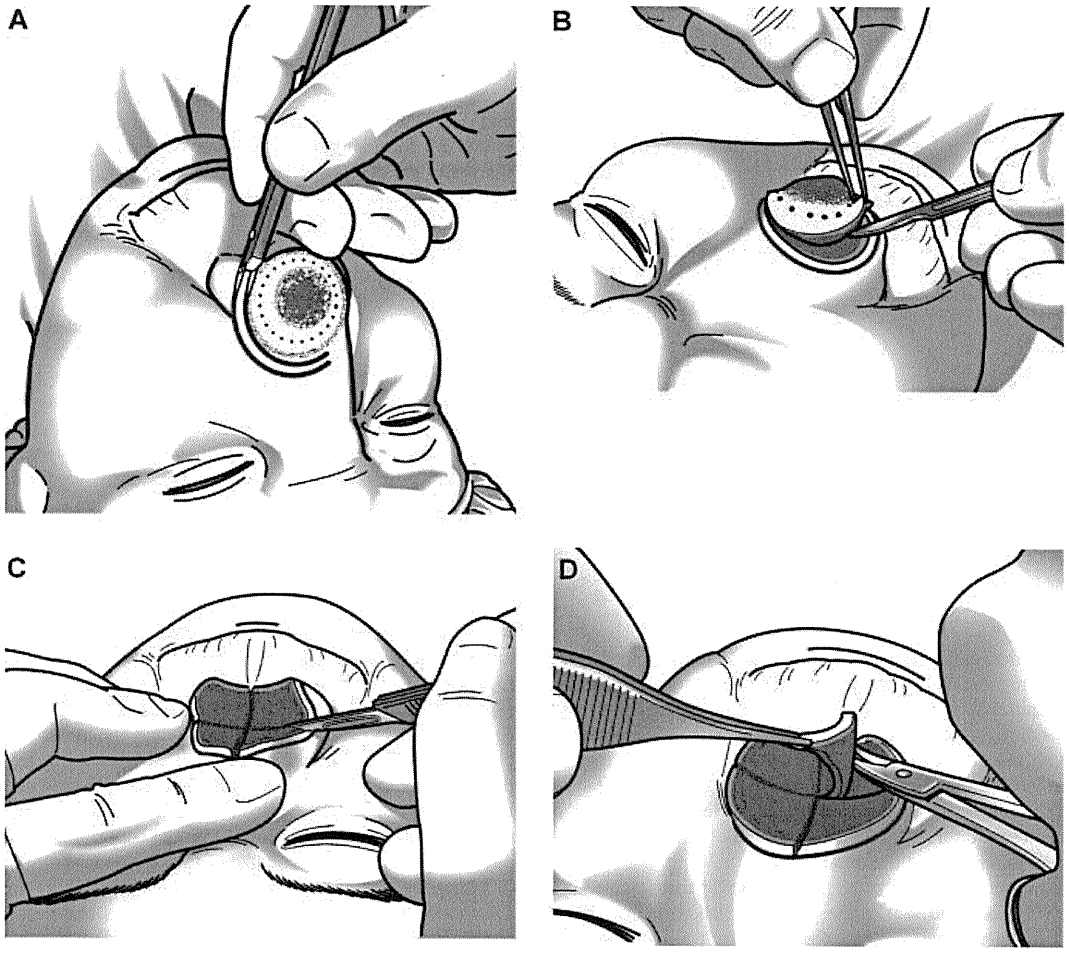

Fig. 2. Schematic diagrams of our technique. **A**: Using a DBS, parallel excisions are made around the tumor. **B**: The gross tumor with initial surgical margin is excised in a bowl shape along the DBS inner excision. **C**: The defect is sub-sectioned into two to four regions, varying with tumor size. **D**: An additional layer of tissue along with 2-mm outer strips of the skin made by DBS is excised at a uniform width by scissors as in conventional MMS.

TABLE II. Summary of Results of NMSC Cases Treated by Micrographic Surgery in Our Simple Method for Complete Histological Margin Control

Case	Anesthesia	Total procedure time (min)	Type of reconstruction	Number of re-excision	Initial surgical margin (mm)	Final margin (mm)	Recurrence
1	Local	104	Flap	2	5	7	None
2	Local	89	Flap	1	2	2	None
3	Local	116	Flap	1	3	3	None
4	Local	80	Flap	1	3	3	None
5	Local	132	Flap	1	5	5	None
6	Local	64	Closure	1	10	10	None
7	Local	131	Flap	2	3	7	None
8	Local	124	Flap	2	3	5	None
9	General	133	Flap, skin graft	2	6	12	None
10	General	232	Combination flap, cartilage graft	2	6	10	None
11	General	167	Combination flap, cartilage graft	1	6	6	None
12	Local	58	Closure	1	2	2	None
13	General	151	Flap	1	7	7	None
14	Local	107	Flap	1	4	4	None
15	Local	170	Combination flap	2	4	9	None